Journal Pre-proof

Thermochronology of South America passive margin between Uruguay and southern Brazil: A lengthy and complex cooling history based on (U–Th)/He and fission tracks

João Pacífico Machado, Andréa Ritter Jelinek, Randell Stephenson, Paul O'Sullivan

PII: S0895-9811(20)30562-9

DOI: https://doi.org/10.1016/j.jsames.2020.103019

Reference: SAMES 103019

To appear in: *Journal of South American Earth Sciences*

Received Date: 1 June 2020

Revised Date: 9 October 2020

Accepted Date: 5 November 2020

Please cite this article as: Machado, Joã.Pací., Jelinek, André.Ritter., Stephenson, R., O'Sullivan, P., Thermochronology of South America passive margin between Uruguay and southern Brazil: A lengthy and complex cooling history based on (U–Th)/He and fission tracks, *Journal of South American Earth Sciences* (2020), doi: https://doi.org/10.1016/j.jsames.2020.103019.

Credit Author statement

João Pacífico S. L. Machado – Conceptualization; Methodology; Formal analysis; Investigation; Writing -Original Draft; Visualization; Project administration; Funding acquisition

Andréa Ritter Jelinek – Conceptualization; Investigation; Writing - Review & Editing; Supervision; Funding acquisition

Randell Stephenson – Conceptualization; Writing - Review & Editing; Supervision; Funding acquisition

Paul O'Sullivan – Methodology; Formal analysis; Investigation; Writing - Review & Editing

Thermochronology of South America passive margin between Uruguay and southern Brazil: a lengthy and complex cooling history based on (U-Th)/He and fission tracks

João Pacífico Machado [1]*, Andréa Ritter Jelinek [2], Randell Stephenson [1], Paul O'Sullivan [3]

1 School of Geosciences, University of Aberdeen, United Kingdom

2 Instituto de Geociências, Universidade Federal do Rio Grande do Sul, Brazil

3 GeoSep Services, United States

* Correspondence (j.luizmachado.18@abdn.ac.uk)

ABSTRACT

Thermochronology studies carried out in crystalline rocks on the South America passive margin reveal distinct cooling patterns along the coast. While most of the margin presents syn- to post-rift final exhumation, the region between parallels 29° and 35° S presents primarily pre-rift exhumation. This stretch of the coast corresponds to Uruguay and southern Brazil, where the Rio de La Plata Craton and the Dom Feliciano Belt occur. Previous studies in the area suggest temperatures below 200 °C since the early Paleozoic, and a complex thermotectonic history during the Phanerozoic. Here we present the first zircon fission track ages for both craton and belt; they range between 562 and 280 Ma and corroborate an early Paleozoic cooling of the basement, likely related to regional exhumation after the Brasiliano/Pan-African Cycle (Neoproterozoic-Cambrian) and the formation of West Gondwana. The thermal history after this cooling phase is a matter of debate. Therefore, we compiled all thermochronometry ages available for the region to evaluate the current hypotheses for the basement exhumation. We suggest that this region went through protracted and continuous cooling during the Paleozoic-Mesozoic, until South Atlantic opening in the Jurassic-Cretaceous. The basement was exposed to near surface conditions (T ≤ 60 °C) in the Mesozoic, and the magmatism associated with the breakup likely caused a geothermal disturbance, which may be responsible for the highly dispersed apatite (U-Th)/He ages observed in previous studies. Basement exhumation after South Atlantic opening was minimal in the region. The key to constrain the low temperature thermotectonic history of both craton and belt appears to be a better comprehension of the long-term effects of accumulation of radiation damage within thermochronometers, and to quantify the effects of protracted cooling and minor reheating events on apatites and zircons with variable uranium content.

KEYWORDS

Fission tracks; (U-Th)/He; South Atlantic rift; West Gondwana; Rio de La Plata Craton; Dom Feliciano Belt.

1 Introduction

Low-temperature thermochronometry has the potential to unveil the thermal history of rocks at temperatures below *c.* 250 °C, or in other words, the thermal history of the shallow crust. The integration of distinct thermochronometers, i.e. sets of mineral and radiogenic systems which record cooling through a specific range of temperature, allows investigation of phases of cooling and heating of the shallow crust, which can be linked to tectonic and magmatic events on various scales. This research method has helped to understand the geodynamics in different active settings, as in the development of mountain ranges (e.g. O'Sullivan et al. 1997; Parra et al. 2009), the dislocation of fault zones (e.g. Tagami 2012), and the emplacement of hydrothermal mineral deposits (e.g. Jelinek et al. 2003). Simultaneously, the method has also been successful when applied to geotectonic settings known for their long-term stability, such as cratons (e.g. Flowers 2009; Kasanzu 2017) and passive margins (e.g. Gallagher et al. 1994; Wildman et al. 2016), providing valuable insights about the thermotectonic behavior of these tectonically dormant regions.

The South Atlantic passive margin, between latitudes 35°S and 29°S, is one of these stable regions that has been investigated by thermochronometry in the last decades (de Borba et al. 2002, 2003; Bicca et al. 2013; de Oliveira et al. 2016; Kollenz 2015; Hueck et al. 2017, 2019; Gomes & Almeida 2019; Machado et al 2019, 2020). This region runs from Uruguay to southern Brazil, and its basement is composed of two major geotectonic features that are continuous across both countries: the Rio de La Plata Craton and the Dom Feliciano Belt (Fig. 1). During the Brasiliano/Pan-African Cycle (Neoproterozoic to Cambrian), the West Gondwana megacontinent formed in response to diachronic terrane accretions and collisions between the Rio de La Plata, Congo and Kalahari cratons, which led to the creation of the Dom Feliciano Belt and the consolidation of the region in the central part of the megacontinent (Cordani et al. 1968; de Brito Neves & Fuck 2013; Oriolo et al. 2017). About 400 Ma later, the Dom Feliciano Belt, characterized by NE-SW trending structures, became the *locus* of the South Atlantic rifting, which propagated northwards following inherited lithospheric zones of weakness that originally formed during the Brasiliano/Pan-African Cycle (Buiter & Torsvik 2014; Will & Frimmel 2018). Therefore, for most of the Phanerozoic, between the final amalgamation of South America and Africa (Cambrian) and the opening of the South Atlantic Ocean (Jurassic/Cretaceous), this region was in an intracontinental setting (Scotese et al. 1999), distant from active margins, thus less susceptible to vertical movements of the crust.

Subsequently, during the breakup of West Gondwana and opening of the South Atlantic Ocean, the region was prone to significant vertical movements of the crust, more easily recorded by thermochronometers as cooling/heating episodes.

Nevertheless, the aforementioned thermochronometry studies carried out in Uruguay and southern Brazil suggest a complex Phanerozoic thermotectonic history for the region. The basement's main cooling phase and uplift preceded the Cretaceous continental rupture, and the possible reheating phase(s) are poorly constrained by the current models. In addition, the causes and geodynamic forces driving such a thermal history are a matter of debate. Different studies have correlated the cooling/heating phases to (1) collisions and accretions in the active SW margin of West Gondwana (e.g. de Borba et al. 2002, 2003; de Oliveira et al. 2016; Machado et al 2019, 2020), (2) the depositional cycles of the intracratonic Paraná Basin (e.g. de Borba et al. 2002, 2003; Kollenz 2015; Hueck et al. 2017, 2019), and to (3) mantle processes and the opening of the South Atlantic Ocean (e.g. Bicca et al. 2013; Gomes & Almeida, 2019; Hueck et al. 2019; Machado et al. 2019, 2020).

In this study we review the previous thermochronometry results from the region, focusing on the data obtained from basement samples from both the Rio de La Plata Craton and the Dom Feliciano Belt, between Uruguay to southern Brazil. Furthermore, eighteen new zircon fission track ages and two apatite (U-Th)/He ages are presented, and integrated with the published low-temperature thermochronometry data, in order to provide further details constraining the region's thermal history. The proposed thermal histories from 77 apatite fission track samples collected across the basement, and modeled by their different authors, are compiled into interpolation maps, allowing the visualization of the cooling trends of the region since the Devonian. Finally, there is a discussion of the current interpretations for the thermal history of the regional basement, which indicates that there are still open questions to be answered in the region.

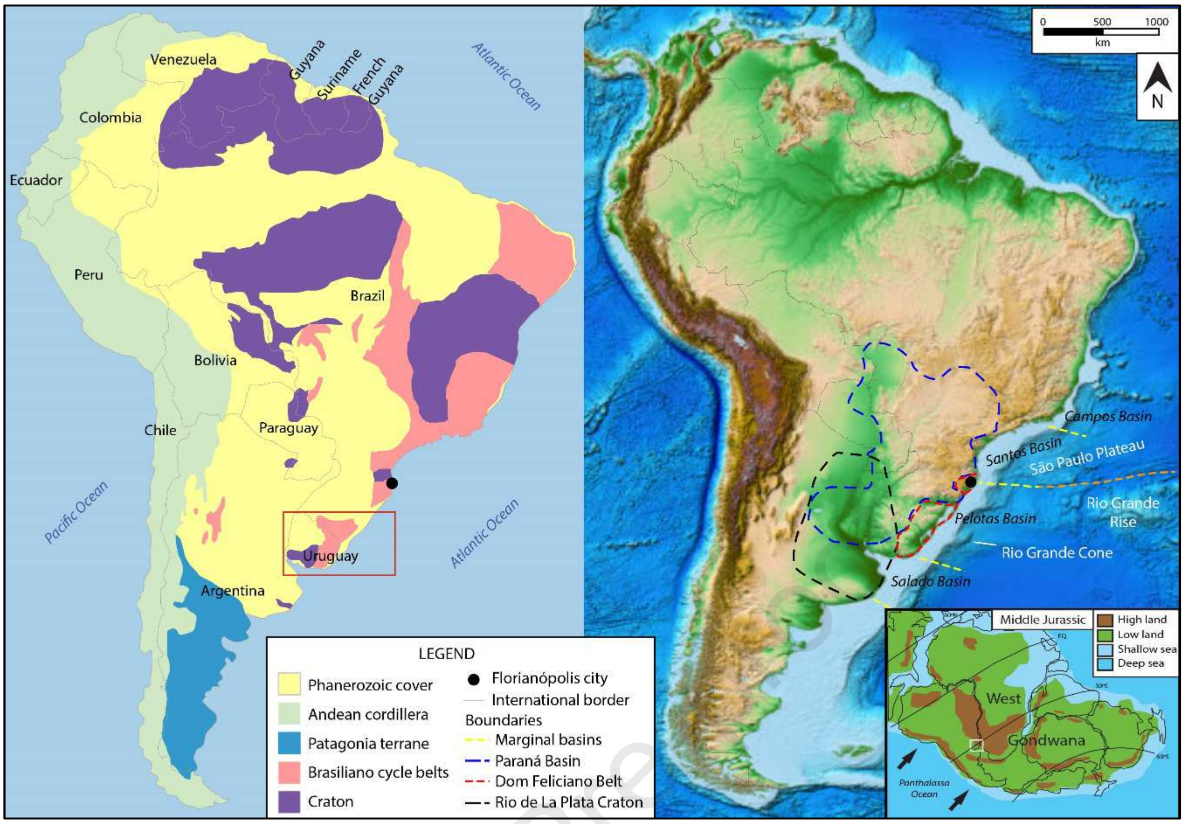

Figure 1: Left, main geotectonic features in South America, with the study region marked by the red rectangle. On the right, the approximated limits of the Rio de La Plata Craton, Dom Feliciano Belt, Paraná and marginal basins, as well as some bathymetric highs in the Atlantic Ocean. Inset map indicates the study area (white square) before West Gondwana breakup. Modified from Scotese et al. (1999), Hartmann et al. (2001) and Amante & Eakins (2009). FORMAT SUGGESTION: 2 columns wide.

2 Geological setting

2.1 Precambrian basement and West Gondwana amalgamation

The basement in the study area comprises two major geotectonic units that run from Argentina to southern Brazil: the Rio de La Plata Craton and the Dom Feliciano Belt (Figs. 1 and 2). The region was consolidated after the Brasiliano/Pan-African Cycle (Neoproterozoic to Cambrian), a protracted orogenic cycle that involved the closure of oceans, collision of cratons and accretion of several microcontinents and volcanic arcs. This cycle is part of the formation of the West Gondwana megacontinent, with the amalgamation of what would become South America and Africa (de Almeida et al. 1981; de Brito Neves et al. 2014). Despite frequent changes in the stress fields during the diachronic collisions between the different crustal blocks, the structures along the southeast margin of South America generally show NE-SW strike, including thrust faults and transcurrent shear zones of ductile and brittle deformation (de Almeida et al. 1981; Hasui 2010; de Brito Neves et al. 2014). After the final amalgamation of West Gondwana, the region went through a stabilization phase that lasted most of the

Paleozoic, dominated by weathering and erosion, and correlated to the development of the intracontinental Paraná Basin (Milani & Ramos 1998; Hackspacher *et al.* 2004; Hasui 2010). This stability stage lasted until the Early Jurassic, when the onset of West Gondwana breakup, which caused the reactivation of inherited basement structures and resulted in the Early Cretaceous opening of the South Atlantic Ocean from south to north (Buiter & Torsvik 2014; Will & Frimmel 2017).

In the study area, the Rio de La Plata Craton and the Dom Feliciano Belt are subdivided into eight tectonostratigraphic terranes bounded by regional shear zones (Fig. 2). The craton consists of the Piedra Alta (UY) and Tandilla (UY) terranes in the west and, arguably, the Nico Pérez (UY) and Taquarembó (BR) terranes in the middle. In the east, the Dom Feliciano Belt is divided into the São Gabriel (BR) and Tijucas (BR) terranes, plus the Pelotas Batholith (BR) and the Cuchilla Dionísio Terrane (UY) in the easternmost part of the belt (Gaucher et al. 2011; Rapela et al. 2011; Oyhantçabal et al. 2011; Philipp et al. 2016).

The main exposure of the Rio de La Plata Craton, the Piedra Alta Terrane, is a Paleoproterozoic block (2.2 to 2.0 Ga) composed of a central granitic gneiss belt bordered in the south and north by low-grade metamorphic belts, and intruded by a dike swarm around 1.79 Ga (Teixeira et al. 1999; Hartmann et al. 2001). The Tandilia Terrane comprises Paleoproterozoic granitoids and a medium-grade schist belt, being continuous southwards along the coast, cropping out again in Argentina (Hartmann et al. 2002; Gaucher et al. 2008; Bossi & Cingolani 2009). The Nico Pérez Terrane, and its continuation in Brazil, the Taquarembó Terrane, represents the most complex unit in the region, and the timing of its accretion to the rest of the Rio de La Plata Craton is controversial. This unit was sutured to the craton either in the Neoproterozoic (Oriolo et al., 2016; Oyhantçabal et al. 2018) or in the Mesoproterozoic (Gaucher et al. 2008, 2011; Santos et al. 2017), and was reworked during the Brasiliano/Pan-African Cycle (Oyhantçabal et al. 2011; Santos et al. 2017). Nevertheless, the Nico Pérez and Taquarembó terranes comprise magmatic-metamorphic complexes and metavolcanic-sedimentary sequences in an intricate arrangement, with ages of the main lithologies ranging from the Archean to the Cambrian, and alkaline magmatism up to Cretaceous age (Hartmann et al. 2001; Oyhantçabal et al. 2012; Oriolo et al. 2016; Gaucher et al. 2016).

Located in the northwest part of the Dom Feliciano Belt, the São Gabriel Terrane corresponds to a juvenile association of magmatic arcs and ophiolite slabs, representative of the early stages of the Brasiliano/Pan-African Cycle, and intruded by post-orogenic granites (Hartmann et al. 2007; Philipp et al. 2016). The Tijucas Terrane comprises Neoproterozoic metavolcanic-sedimentary sequences with Archean inliers and Cretaceous alkaline magmatism

(Barbieri et al. 1987; Chemale 2000; Hartmann et al. 2007). The Pelotas Batholith, named the Aiguá Batholith in Uruguay, is composed mostly of calc-alkaline intrusive suites emplaced between 650 Ma and 530 Ma, largely under the influence of the NE-SW shear zones (Chemale 2000; Philipp *et al.* 2003, 2016).The Cuchilla Dionísio Terrane includes a high-grade metamorphic basement and metasediments with affinity to the Kalahari Craton, being considered an allochthonous unit (Bossi & Gaucher 2004; Basei et al. 2005, 2011.)

Finally, the crystalline basement is partially covered by remnants of the Camaquã Basin, in Brazil, and of the Arroyo del Soldado Group, in Uruguay. Both were deposited in late to post-orogenic settings, between the Ediacaran and Cambrian, with units of the Camaquã Basin providing a minimum depositional age of 473 ± 9 Ma (Blanco *et al.* 2009; Maraschin *et al.* 2010; de Oliveira *et al.* 2014).

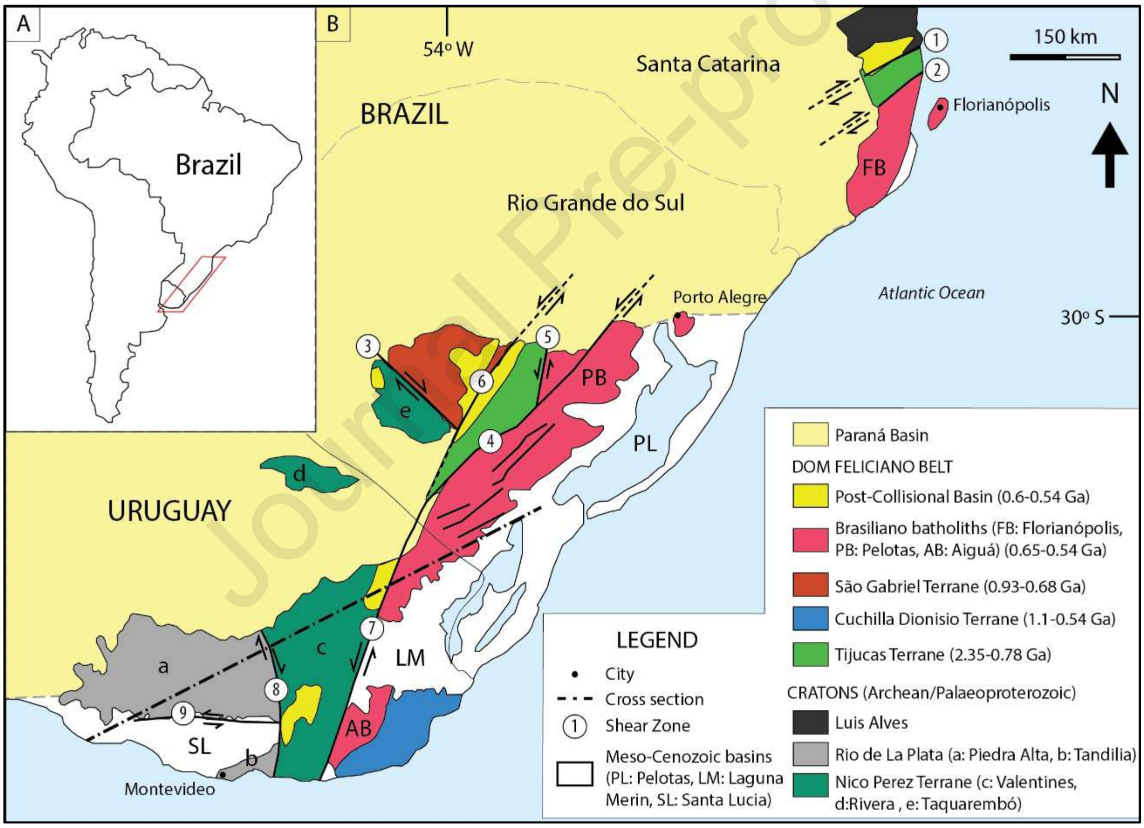

Figure 2: Tectonostratigraphic terranes and volcanic-sedimentary cover in the region of interest. Main faults and shear zones: 1) Itajaí-Perimbó, 2) Major Gercino, 3) Ibaré, 4) Dorsal de Canguçu, 5) Passo do Marinheiro, 6) Caçapava, 7) Sierra Ballena, 8) Sarandí del Yí, 9) Colônia. Modified after Chemale (2000) and Phillip et al. (2016). FORMAT SUGGESTION: 2 columns wide.

2.2 Phanerozoic cover and West Gondwana breakup

The basement exposures in Uruguay and southernmost Brazil are surrounded mainly by the Paleozoic and Mesozoic deposits of the Paraná Basin. In turn, the Atlantic margin is the domain of the Meso-Cenozoic Pelotas Basin, formed as a consequence of continental breakup.

South Atlantic opening is also related to the formation of two minor basins in Uruguay, the Santa Lucia and Laguna Merin basins.

The Paraná Basin is a broad intracontinental basin that spreads over Argentina, Brazil, Paraguay and Uruguay (Fig. 1), and was developed in the interior of West Gondwana during the Paleozoic and Mesozoic. The depositional succession within this basin is divided into six supersequences separated by interregional unconformities: Rio Ivaí (Ordovician to Silurian), Paraná (Devonian), Gondwana I (Upper Carboniferous to Lower Triassic), Gondwana II (Middle to Upper Triassic), Gondwana III (Jurassic to Lower Cretaceous), and Bauru (Upper Cretaceous) (Milani 1997; Milani et al. 2007). In the study area units from the Paraná to the Gondwana III supersequences are exposed. The Gondwana III supersequence was deposited immediately before West Gondwana breakup and comprises the Botucatu Formation, characterized by highly quartzose aeolian sandstones (Scherer 2000; Bertolini et al 2020), and the Serra Geral Formation, which is essentially a basaltic sequence that covers the Botucatu paleodesert. The Serra Geral Formation occurs over more than 1 million km^2 and can reach a thickness of more than 1.500 m, representing the volcanism of the Paraná-Etendeka Large Igneous Province (LIP), with a peak at *c.* 134 Ma (Turner et al. 1994; Ponte & Asmus 2004; Rossetti et al. 2014).

The Pelotas Basin is a passive marginal basin developed during the Atlantic Ocean opening (Fig. 2), which presents abundant siliciclastic sediments, mostly fine grained, while lacking extensive evaporite deposits (Dias et al. 1994; Bueno et al. 2007). The lowermost formations of the basin are related to the Mesozoic rifting and characterized by intense magmatism, which has formed thick wedges of seaward-dipping reflectors (Gladczenko et al. 1997; McDermott et al. 2019). From the Cretaceous onwards, the sedimentation is mostly siliciclastic, with some carbonate formations in the early stages (Dias et al. 1994; Beglinger et al. 2012). The tectonic stress associated with the West Gondwana breakup and the Atlantic opening led to the formation of two other basins onshore in Uruguay, named the Santa Lucia and Laguna Merin basins (Fig. 2). These two basins form an ENE-WSW structural corridor known as SaLAM, that is considered an aborted rift precursor to the opening of the South Atlantic during the Jurassic-Cretaceous (Rossello *et al.* 2000, 2007). Despite the genetic link, the two basins exhibit very distinct volcanic-sedimentary infill and are separated by a basement high represented by the Nico Pérez Terrane, where only a few remnants of volcanic deposits are found (Rossello *et al.* 2000). The Santa Lucia Basin corresponds to the SW part of the SaLAM, presents a central structural high with E-W strike and comprises mostly siliciclastic deposits, reaching a total thickness of 2.500 m (Rossello et al. 2000; Veroslavsky et al. 2003). The NE SaLAM is represented by the Laguna Merin Basin, which is mainly composed of volcanic rocks with ages between 134 to 127 Ma and covered by Cenozoic sedimentary rocks (Cernuschi et al. 2015).

Continental breakup was diachronous between South America and Africa, with South Atlantic rifting starting in Argentina in the Jurassic and propagating northwards thereafter (Mizusaki et al. 1988; Stica et al. 2014). In the study area, the breakup is marked by extensive igneous activity in the Paraná Basin and in the forming marginal Pelotas Basin, with volcanism closely preceding or being concomitant to the South Atlantic opening (Mohriak 2012). The causes and mechanisms of rifting remain under debate, but there is general agreement that mantle dynamics were involved. The onset of rifting is often related to the presence of the Tristan da Cunha mantle plume, initial emplacement of which under the South American plate is linked to the magmatism of the Paraná-Etendeka LIP (e.g. Chang et al. 1992; Brown et al. 2000; Pérez-Diaz & Eagles 2014; Buiter & Torsvik 2014).

During the breakup, the South American margin was hyperextended with substantial crustal thinning, exhumation of the mantle/lower crust and doming related to the influence of the mantle plume, leading to topographic elevation until the final rupture (Aslanian et al. 2009; Mohriak 2012). The breakup also involved ridge jumps eastwards, while the northwestwards movement of the South American plate is marked by a NW-SE trend of bathymetric highs along the oceanic floor, most likely the result of the lithosphere passing over the mantle plume (Nurnberg & Muller 1991; Mohriak *et al.* 2010; Brown *et al.* 2000; Graça *et al.* 2019). The study area is located between large magmatic bodies: to the north and west the voluminous volcanic deposits of the Paraná-Etendeka LIP in the Paraná Basin, and to the east and southeast the thick wedges of the seaward-dipping reflectors in the Pelotas Basin (Gladczenko et al. 1997; Rossetti et al. 2014; McDermott et al. 2019). Additionally, remote sensing surveys revealed a dyke swarm cutting through southernmost Brazil and Uruguay, which most likely is related to the LIP (Hartmann et al. 2016; Demarco et al. 2020). Magmatism continued until the Campanian (Late Cretaceous), with the emplacement of phonolitic plugs in southernmost Brazil (between 99 and 76 Ma) (Barbieri et al. 1987) and subalkaline rhyolites in Uruguay (77 ± 1 Ma) (Gaucher et al. 2016). Therefore, the study area was directly affected by the magmatism pre-, syn- and post-rift, being exposed to the thermal effects of these events over long periods of time.

3 Methods

3.1 Thermochronometry analyses

In this study we evaluate data from four low-temperature thermochronometers and publish new ages for two. The zircon fission track (ZFT) method records the time at which a sample cools to temperatures below *c.* 240 ± 40 °C, under which the fission tracks are preserved within the zircon crystal lattice (Hurford 1986; Bernet et al. 2004; Bernet & Garver 2005). However, the partial annealing zone, in which tracks are slowly shortened (annealed), and the blocking temperature of this method, below which tracks are preserved with their original length, are sensitive to the cooling history and damage accumulated within the crystal (Tagami 2005; Bernet & Garver 2005; Yamada et al. 2007; Marsellos & Garver 2010). Therefore, ZFT ages provide valuable insights on the cooling history of the sample, especially if combined with other thermochronometers. Hence, the ZFT ages presented here are compared to ages from other thermochronometers, specially with zircon (U-Th/He) ages (ZHe) obtained in previous studies (Hueck et al. 2017, 2019; Machado et al. 2019, 2020), and which presents a slightly lower temperature sensitivity, between *c.* 190 and 150 °C (Reiners et al. 2017). We also integrate the new ZFT ages with data from apatite fission track (AFT) analysis, which records temperatures between *c.* 110 and 60 °C, and apatite (U-Th)/He (AHe), sensitive to temperatures between *c*. 70 and 40 °C (Gleadow et al. 1986; Wagner et al., 1989; Wolf et al. 1996, 1998; Reiners et al. 2017).

For the ZFT analysis, we used basement samples from the Rio de La Plata Craton (n=9) and the Dom Feliciano Belt (n=9), from the same locations as Machado et al. (2019, 2020). Analysis were performed at GeoSep Services by Paul O'Sullivan using standard procedures for the laser-ablation inductively-coupled plasma mass spectrometer (LA-ICP-MS) method. See Donelick et al. (2005), Hasebe et al. (2004, 2013) and Congné et al (2020) for a full description of analytical procedures, and the Supplementary Material for specific LA-ICP-MS operating conditions and data acquisition parameters. Zircon crystals were mounted in FEP Teflon and polished to expose internal crystal surfaces. Mounts were immersed in a eutectic melt of NaOH+KOH at 210 °C (±10 °C) for between 8 and 24 hours to reveal naturally occurring fission tracks. The polished and etched zircon crystals surfaces were then cleaned in reagent-grade 48% HF for 15 minutes at 23 °C. Spontaneous tracks were counted on the zircon mounts in unpolarized light at 2000x magnification, from crystals selected to sample the greatest range of observable characteristics (size, degree of roundness, color, etch figure size, etc.). A LA-ICP-MS was then used to determine the ^{238}U concentrations by measuring the ratio of ^{238}U to ^{29}Si for zircon, from the exact regions on the individual crystals from which the spontaneous tracks were initially counted. An Agilent 7700 high resolution single-collector ICP-MS equipped with a New Wave Nd-YAG 213nm laser ablation system at Washington State University was used for this purpose. In order to increase our area coverage, sample ages were calculated from 10 single-crystal analyses instead of the more usual 20-25 single-crystals. This approach potentially reduces the data reliability and limits our interpretations. To compensate for the reduced dataset and evaluate the reliability of the new ZFT ages, from the 18 analyses, seven were made in samples with published ZHe ages, which allowed comparison of the ages from two thermochronometers with contiguous thermal sensitivity (ZHe and ZFT) in seven locations. It was then possible to compare the ZFT ages from these double-dated locations to the ZFT ages obtained from other samples within the same tectonostratigraphic terrane but without previous ZHe data. Although unconventional, our approach allowed coverage over a vast area and provided satisfactory results when compared to previous thermochronometry studies in the region. The ZFT single-crystal and pooled ages were calculated using the scheme presented by Donelick et al. (2005) and a modified zeta calibration approach after Hurford and Green (1983; see also Hasabe et al. 2004, 2013; Cogné et al. 2020). The software RadialPlotter 9.5 (Vermeesch, 2009) was used to calculate the central ages, run the chi-square test and generate the radial plots, which can be found in the Supplementary Material.

For the AHe analysis we used two samples from the northern part of the Pelotas Batholith. Analyses were performed in the (U-Th)/He and U-Pb Geo-Thermochronology Laboratory of the University of Texas at Austin, by Andréa Jelinek. AHe ages are based on three single crystal ages, from apatites handpicked and screened for inclusions using a Nikon SMZ-U/100 stereomicroscope, with transmitted (polarized) and reflected light capabilities. Prior to loading the apatites into Pt sleeves, all crystals were photographed using a Nikon digital ColorView® camera, and the AnalySIS® imaging software was used to morphometrically measure selected apatites. These morphometric values were then used to calculate the alpha-ejection correction particular to each crystal (Farley et al. 1996). The He extraction was made using an automated He Extraction Line for (U-Th)/He dating, and apatite crystals were subsequently recovered for the U and Th measurements after crystal dissolution in a HF-HNO3 mixture. All analytical uncertainties were captured and properly propagated during multi-step and multi-instrument (U-Th)/He analysis, and the AHe age error is based on the reproducibility of the Durango apatite standard.

Further information on the newly presented thermochronometry data as well as on the previously published data that were used in this work can be found in the Supplementary Material.

3.2 Thermochronometry data integration

Apatite and zircon fission track ages (AFT and ZFT), as well as apatite and zircon (U-Th)/He ages (AHe and ZHe) were compiled from de Borba et al. (2002, 2003), Bicca et al. (2013), Kollenz (2015), de Oliveira et al. (2016), Hueck et al. (2017, 2019), Gomes & Almeida (2019) and Machado et al. (2019, 2020). Moreover, the thermal histories published by de Borba et al. (2002, 2003), Kollenz (2015), de Oliveira et al. (2016), Gomes & Almeida (2019) and Machado et al. (2019, 2020), all based on AFT, were used to estimate the temperature history of 77 different locations across the study region. From the compiled dataset, it was possible to create interpolation maps of the AFT and ZFT ages (Fig. 3), as well of basement temperature since the Devonian (Fig. 5).

From each published model, the mean path of the thermal history was used to estimate the temperature of the location at eight specific times (see Supplementary Material for the locations and temperatures used in each interpolation). Temperature maps for the middle Paleozoic have less data for interpolation because some of thermal models used did not register the sample’s temperature that far in the past. The lowest number of thermal models used for the interpolations corresponds to 48 locations, which were used to estimate temperature 400 Ma ago. Interpolations for ages younger than this are based on a progressively increasing number of thermal models, up to the 77 locations for the 150 Ma and younger interpolations. It is noteworthy that the temperatures used in the interpolation maps were obtained from the mean path of thermal model of each location. Hence, the temperature range at each location at a specific age varies according to how well constrained the thermal model is. In general, temperatures are better constrained at younger ages, but the variation can easily be of ± 10 °C, or even more. Thus, it is not possible to distinguish small variations in the location`s temperature. In any case, the interpolation of the 77 thermal histories modeled independently by different authors, on different software and with different data and constraints provide valuable insights on the general thermal history of both craton and belt. The contour maps presented here were created using the kriging interpolation method on Surfer 13.6, and then imported into ArcMap 10 for georeferencing and cropping into the limits of the basement in the region.

4 Results

4.1 Fission track ages

We obtained eighteen ZFT ages, nine from the Rio de La Plata Craton (Piedra Alta, Tandilia and Nico Pérez terranes) and nine from the Dom Feliciano Belt (Pelotas Batholith and

Cuchilla Dionísio Terrane) (Table 1). Considering the entire basement, ZFT pooled ages range between 530-254 Ma while the central ages range between 562-280 Ma, and both are indistinguishable within analytical uncertainties. Also, there is a fair similarity among ages from samples within the same tectonostratigraphic terrane (Fig. 3). In the dataset, it is notable the somewhat young pooled ages in the Rio de La Plata Craton *stricto sensu* (Piedra Alta and Tandilia terranes), that range between 354-297 Ma. Meanwhile, the Nico Pérez Terrane, arguably part of the craton, presents older pooled ages, between 527-468 Ma. A similar pattern is observed within the central ages from these terranes. However, samples from the Piedra Alta Terrane failed the chi-square test ($P(\chi2)$ <5%) and show considerable single-grain age dispersion, which appears to be related to the radiation damage accumulated within each single zircon, discussed in section 5.1. Besides the samples from the Piedra Alta Terrane, only one more sample (RS07 from the Pelotas Batholith) failed the chi-square test, but it shows similar age to other nearby samples. Therefore, the majority of our samples have one age population with a Poisson distribution, as could be expected for ZFT ages from basement samples. Concurrently, to the east, the Dom Feliciano Belt presents ZFT pooled ages between 530-254 Ma and central ages between 550-280 Ma; this range is characteristic of the Cuchilla Dionísio Terrane, in the southeastern part of the belt. The ZFT ages from the Pelotas Batholith are more uniform: pooled ones range from 464 to 437 Ma and central ones from 500 to 463, which indicates a regional cooling pattern for the batholith, spreading over more than 300 km along the margin. Meanwhile, the easternmost samples from the Cuchilla Dionísio Terrane have late Paleozoic ages (*c.* 280 Ma), but the southeasternmost sample presents an early Paleozoic age around 540 Ma. This region also presents older AFT ages when compared to the ones to northeast along the coast (Fig. 3), which suggests an early cooling of the southern part of Cuchilla Dionisio Terrane.

Finally, the 97 AFT central ages compiled from de Borba et al. (2002, 2003), Bicca et al. (2013), Kollenz (2015), de Oliveira et al. (2016), Gomes & Almeida (2019) and Machado et al. (2019, 2020) range from 383 ± 40 to 74 ± 5 Ma, of which 74 ages are Mesozoic, mostly Jurassic. Ages tend to be younger towards the east and northeast on the study region. This AFT dataset suggests that both craton and belt cooled below 60 °C during the Mesozoic, with the western region reaching lower temperatures before the eastern one (Fig. 3).

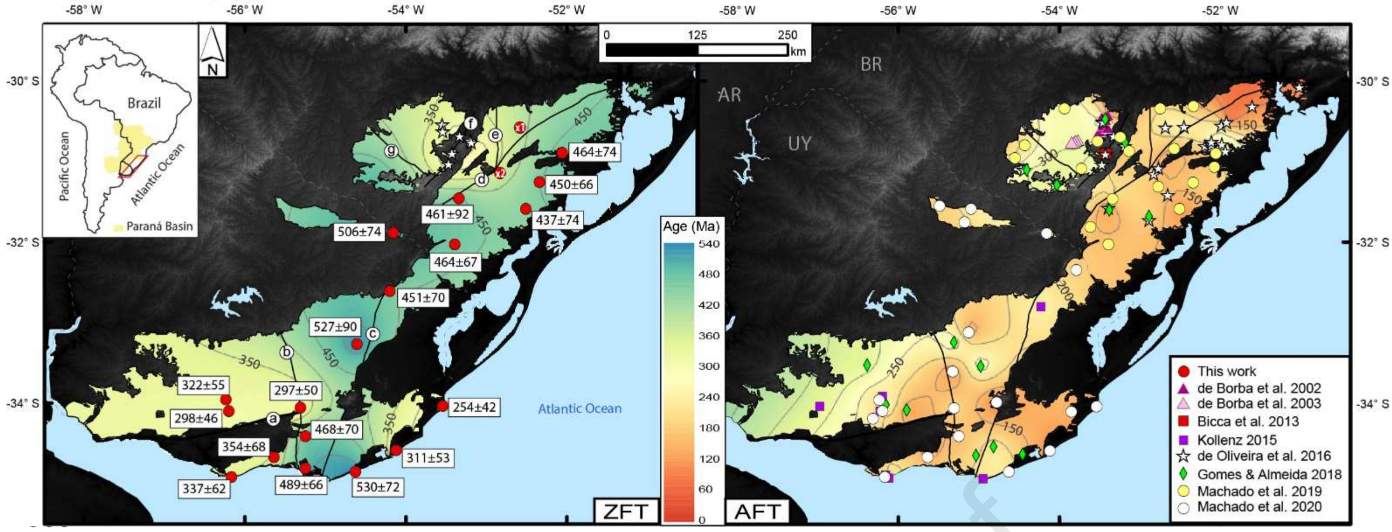

Figure 3: Left, new zircon fission track pooled ages and contour map of all ZFT ages available in the region (n=25). Note the younger ages from de Oliveira et al. (2016) at north, and the ones located in the Piedra Alta and Tandilia terranes, southwest, as well as in the east coast of Uruguay. In the north of the Pelotas Batholith, the “X1” and “X2” mark the locations of the two new AHe ages presented here. Right, contour map of apatite fission track ages in the region (n=97). Note the older AFT ages in the Piedra Alta, Taquarembó and São Gabriel terranes, and the trend of younger ages towards the east and northeast along the margin. Shear zones: a) Colônia, b) Sarandí del Yí, c) Sierra Ballena, d) Dorsal de Canguçu, e) Passo do Marinheiro, f) Caçapava, g) Ibaré. FORMAT SUGGESTION: 2 columns wide.

Table 1: Summary of Zircon Fission Track results obtained for the Rio de La Plata Craton and the Dom Feliciano Belt, using the LA-ICP-MS method. Pooled and Central ages are reported, calculated using a primary zeta of 0,0401 ± 0,0005 based on Fish Canyon Tuff standard. N, number of crystals analyzed; χ2, chi-square probability of single population.

Zircon Fission Track analyses															
Sample #	Lat (°)	Long (°)	Elevation (m)	Lithology type	N #	Pooled age (Ma)	-95% (Ma)	+95% (Ma)	Central age (Ma)	±1σ (Ma)	χ2 (%)	Mean U (ppm)	Mean Th (ppm)	Mean Sm (ppm)
Rio de La Plata Craton														
Piedra Alta Terrane														
UY16	-34.06	-55.31	266	Granite	10	297.5	43	50	450	98	0	114.4	148.1	20.3
UY26	-34.10	-56.20	47	Granite	10	298.5	40	46	357	48	5	147.2	49.2	38.6
UY27	-33.96	-56.24	133	Granite	10	322.2	48	56	484	99	0	119.1	124.4	37.1
Tandilia Terrane														
UY18	-34.06	-55.31	266	Gneiss	8	337.4	53	63	385	46	50	84.6	74.5	15.0
UY19	-34.92	-56.17	150	Granite	10	354.1	58	69	426	48	37	28.7	20.7	16.1
Nico Pérez Terrane														
UY1	-31.89	-54.16	225	Granite	10	506.5	65	74	527	54	96	94.3	81.9	13.7
UY13	-33.28	-54.62	102	Granite	10	527.4	78	91	562	61	100	51.5	77.7	65.7
UY21	-34.41	-55.25	182	Granite	9	468.7	61	70	469	53	100	629.7	233.4	205.6
UY23	-34.81	-55.25	121	Syenite	10	489.2	59	66	487	50	100	70.2	51.5	46.2
Dom Feliciano Belt														
Pelotas Batholith														
RS04	-30.90	-52.06	107	Granite	10	464.2	65	75	479	54	100	61.4	59.4	19.3
RS07	-31.26	-52.34	284	Granite	10	450.3	59	67	494	69	3	115.5	104.0	15.4
RS10	-31.59	-52.51	190	Diorite	10	437.6	57	65	482	49	38	114.0	110.4	15.9
RS12	-31.03	-53.39	285	Granite	10	464.3	59	67	472	50	100	56.8	54.1	15.2
RS14	-31.46	-53.34	426	Granite	7	461.4	78	93	500	65	84	107.4	83.8	17.5
UY3	-32.62	-54.21	256	Mylonite	10	451.3	62	71	463	52	100	85.8	75.0	13.2
Cuchilla Dionísio Terrane														
UY29	-34.85	-54.63	7	Granite	10	530.5	64	73	550	56	46	94.3	81.9	13.7
UY30	-34.59	-54.12	3	Schist	10	311.6	46	53	321	37	100	69.7	47.6	10.3
UY32	-34.04	-53.54	4	Granite	10	254.3	37	43	280	31	67	104.8	89.4	16.4

4.2 (U-Th)/He ages

A total of six apatites from two samples resulted in Middle Triassic to Early Cretaceous AHe ages, uncorrected for Ft, that become Carboniferous to Late Triassic after Ft correction, which takes into account ^{4}He particles that were lost during decay because of alpha-ejection processes (Farley et al. 1996) (Table 2). These new ages do not display a clear correlation with eU (eU = [U] + 0.235 × [Th]) or crystal radius, common parameters used to evaluate (U-Th)/He ages dispersion (Reiners & Farley 2001; Flowers et al. 2007; Brown et al. 2013), but are similar to the AHe ages published by Machado et al. (2019) and Hueck et al. (2019) in the region (Fig. 4). The combination of the new AHe ages with other 139 ZHe and 131 AHe published ages allowed the evaluation of the similarities and differences within the (U-Th)/He thermochronometers in the Rio de La Plata Craton and Dom Feliciano Belt.

Both in the Rio de La Plata Craton and Dom Feliciano Belt, the ZHe ages show a negative correlation with eU, which is observed in all tectonostratigraphic terranes (Fig. 4). This correlation is more evident when the analyzed zircons have a big range of eU content, as is the case of zircons from the Dom Feliciano Belt, which has some crystals with eU > 2500 ppm (Fig. 4B2'). The negative correlation is common in cratonic regions and attributed to a long-term accumulation of radiation damage within the zircons, as crystals with high-eU are prone to develop a highly damaged crystalline lattice over time; this favors ^{4}He diffusivity and loss, resulting in younger ZHe ages (Reiners, 2005; Guenthner et al. 2013). Zircons with low-eU content, hence less affected by radiation damage, present early Paleozoic ZHe ages, suggesting that the basement reached temperatures below *c*. 200 °C by this time. ZHe ages from crystals with eU < 500 ppm appear to be older in the Rio de La Plata Craton than in the Dom Feliciano Belt, which indicate an earlier cooling of the former.

Table 2: Summary of Apatite (U-Th)/He ages and parameters. Crystal dimensions were used to estimate an equivalent spherical radius. eU, total uranium content; Unc., uncorrected; Corr., corrected; Ft, alpha ejection factor for age correction (see Farley et al. 1996).

Apatite (U-Th)/He analyses																		
Sample	Lat	Long	Elevation	Lithology	Crystal	U	Th	Sm	He	eU	Radius	Age Unc.	Ft	Age Corr.	±2σ	Ave. Corr.	±2σ
#	(°)	(°)	(m)	type	#	(ppm)	(ppm)	(ppm)	(nmol/g)	(ppm)	(µm)	(Ma)	#	(Ma)	(Ma)	(Ma)	(Ma)
X1	-30.56	-52.45	440	Granite	1	36.24	53.85	82.63	34.82	49.05	39.40	128.7	0.621	207.2	12.4	217.7	22.4
					2	54.29	91.16	69.64	59.18	75.62	36.20	142.1	0.591	240.1	14.4		
					3	52.26	82.31	141.88	49.47	71.92	37.77	124.7	0.606	205.6	12.3		
X2	-31.15	-52.83	330	Granite	1	86.97	13.69	113.10	96.66	90.69	52.79	193.3	0.725	266.6	16.0	306.7	46.6
					2	28.22	2.35	87.74	39.19	29.20	46.50	241.1	0.693	347.4	20.8		
					3	58.24	5.33	106.28	69.09	60.01	44.42	208.3	0.681	306.1	18.3		

On the other hand, the AHe ages are very dispersed both on the craton and the mobile belt (Fig. 4). The dispersion is observed both intra- and inter-samples, and none of the tectonostratigraphic terranes appears to have their AHe ages straightforwardly controlled by the eU content. It is well known that AHe ages can be affected by several factors, internal or external to each crystal, as for example chemical zonation or ^{4}He implantation from neighboring minerals (see Brown et al. 2013 and Wildman et al. 2016 for a review of these and other factors). But, because the dispersion appears to be the rule in the analyzed samples, it is likely that a more embracing control is responsible for it. The accumulation of radiation damage over a long period is potentially the main factor responsible for the dispersion, as a damaged crystal lattice can favor the retentivity of ^{4}He within the apatites and lead to old AHe ages (Green & Duddy 2006; Shuster et al. 2006). Furthermore, apatites with variable eU and accumulated radiation damage that go through similar thermal histories, with a reheating event not high enough to completely reset the thermochronometer, can present a large span of AHe ages, in which small variations in the maximum temperature cause large differences in the AHe age and eU correlation (Shuster et al. 2006; Fox & Shuster 2014; Reiners et al. 2017).

The integration of data from both thermochronometers ZHe and AHe indicates that the craton and belt have been at low temperatures for prolonged periods of time, which allowed for the accumulation of radiation damage within the crystals. Each thermochronometer responds differently to this accumulation, but in both the observed ages appear to be somehow influenced by the eU content of the minerals. The ZHe ages from low-eU zircons suggest temperatures below 200 °C since the early Paleozoic, while the high-eU zircons suggest a long period at low temperatures to accumulate the radiation damage within the crystals. The AHe age dispersion indicates temperatures below 70 °C since at least the Mesozoic, with dispersion possibly augmented by a reheating event that affected the ^{4}He retention of each apatite individually. Moreover, the main igneous event in the region, the Paraná-Etendeka LIP volcanism (*c.* 134 Ma) (Rossetti et al. 2014), which closely preceded the South Atlantic opening, did not raise the basement temperatures to the point of resetting the AHe ages ($T > 70$ °C).

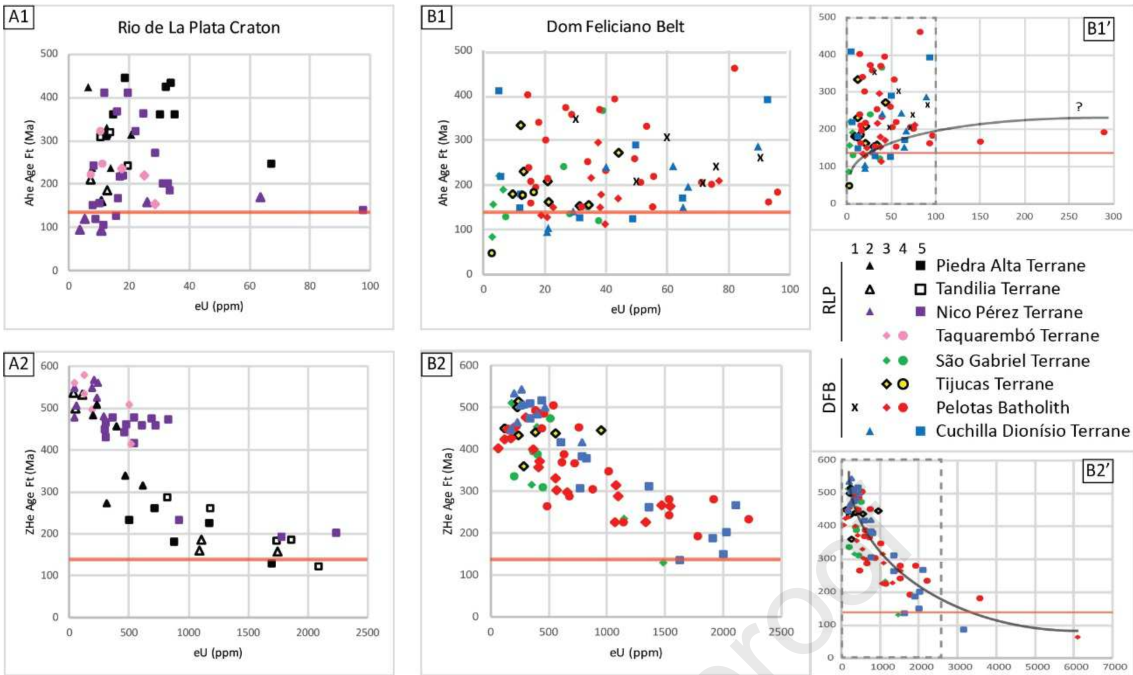

Figure 4: Top row shows plots of AHe ages against eU for the Rio de La Plata Craton (A1) and Dom Feliciano Belt (B1, with inset B1’ which displays trend extrapolation). Bottom row follows the same logic, but for ZHe ages. Note the negative correlation between ZHe ages and eU in both geotectonic units (A2 and B2), and the extrapolated trend observed in the Dom Feliciano Belt, which have a bigger range of eU values (B2’). This negative trend is attributed to a long-term accumulation of radiation damage within the zircons. On the other hand, there is no clear correlation between AHe ages and eU (A1 and B1), and the trend extrapolation for apatites with eU > 100 ppm is unclear (B1’). Red horizontal bar represents the peak of Paraná-Etendeka LIP (134 Ma) (Rossetti et al. 2014). Dashed polygons on B1’ and B2’ indicate the range of B1 and B2 plots. Reported (U-Th)/He ages are Ft corrected and from (1) this work, (2) Hueck et al. 2017, (3) Hueck et al. 2019, (4) Machado et al. 2019, and (5) Machado et al. 2020. FORMAT SUGGESTION: 2 columns wide.

4.3 Basement temperature estimates

The compilation of the thermal histories from 77 locations across the basement, modeled using AFT data sometimes aided by other thermochronometers, allowed estimation of the temperature variation on the region since the Devonian (Fig. 5). Despite a few artifacts observed in the maps that represent locations (i.e. thermal models) with temperatures too different from their surroundings, the interpolation maps permit a qualitative visualization of the cooling trend of the basement.

By the Devonian (400 Ma) most of the basement was already below 160 °C, with the Rio de La Plata Craton registering cooler temperatures when compared to the Dom Feliciano Belt. Around the early Carboniferous (350 Ma) temperatures were near or below 120 °C in most of the basement, with the northeast region, i.e. the Pelotas Batholith, registering the higher temperatures. Some samples near the Sarandi de Yí shear zone, in Uruguay, also present higher temperatures than its surroundings at this time. The interpolation maps for periods younger than the Carboniferous are better constrained and more reliable, because they include 64 locations or more, and because the AFT system is sensitive to temperatures between *c.* 110 to 60 °C (Gleadow et al. 1986; Wagner et al., 1989). During the Carboniferous-Permian transition (300 Ma) temperatures in the craton and belt were mostly below 100 °C, while the Pelotas Batholith to the northeast maintained its higher temperatures when compared to the rest of the basement. This behavior is continuous during cooling through the Permian-Triassic transition (250 Ma) as well during the Triassic-Jurassic one (200 Ma). By the late Jurassic (150 Ma), immediately before the Paraná-Etendeka LIP event (138 to 125 Ma) (Turner et al. 1994; Rossetti et al. 2014), the volcanism in the Laguna Merin Basin (134 to 127 Ma) (Cernuschi et al. 2015) and the opening of the South Atlantic in the region (130 to 113 Ma) (Stica et al. 2014), most of the basement was near or below 60 °C, which indicates that the rocks were exposed or near the surface during the rifting in the region at this time (Jurassic/Cretaceous). The easternmost locations appear to register the highest temperatures at the time of rifting/LIP event, but they usually do not exceed 100 °C. After the South Atlantic opening, at the transition between Early and Late Cretaceous (100 Ma), the basement temperatures were still near 60 °C. The area in the Cuchilla Dionísio Terrane around the volcanic filled Laguna Merin Basin recorded the highest temperatures of the region. Finally, by the Eocene (50 Ma) practically all basement in the region was below 60 °C, with a subtle trend of cooler temperatures towards the hinterland.

This compilation of thermal histories suggests that the terranes which make the Rio de La Plata Craton reached cooler temperatures earlier than the Dom Feliciano Belt. However, there is no straightforward limit on the thermal behavior between these geotectonic units, as the shear zones that cut the basement appear not to have a major influence on the cooling trend of the terranes. Moreover, apparently the magmatism associated with the West Gondwana breakup and South Atlantic opening did not raise the basement temperatures significantly, being responsible at most for maintaining the temperatures near 60 °C during the entire Cretaceous.

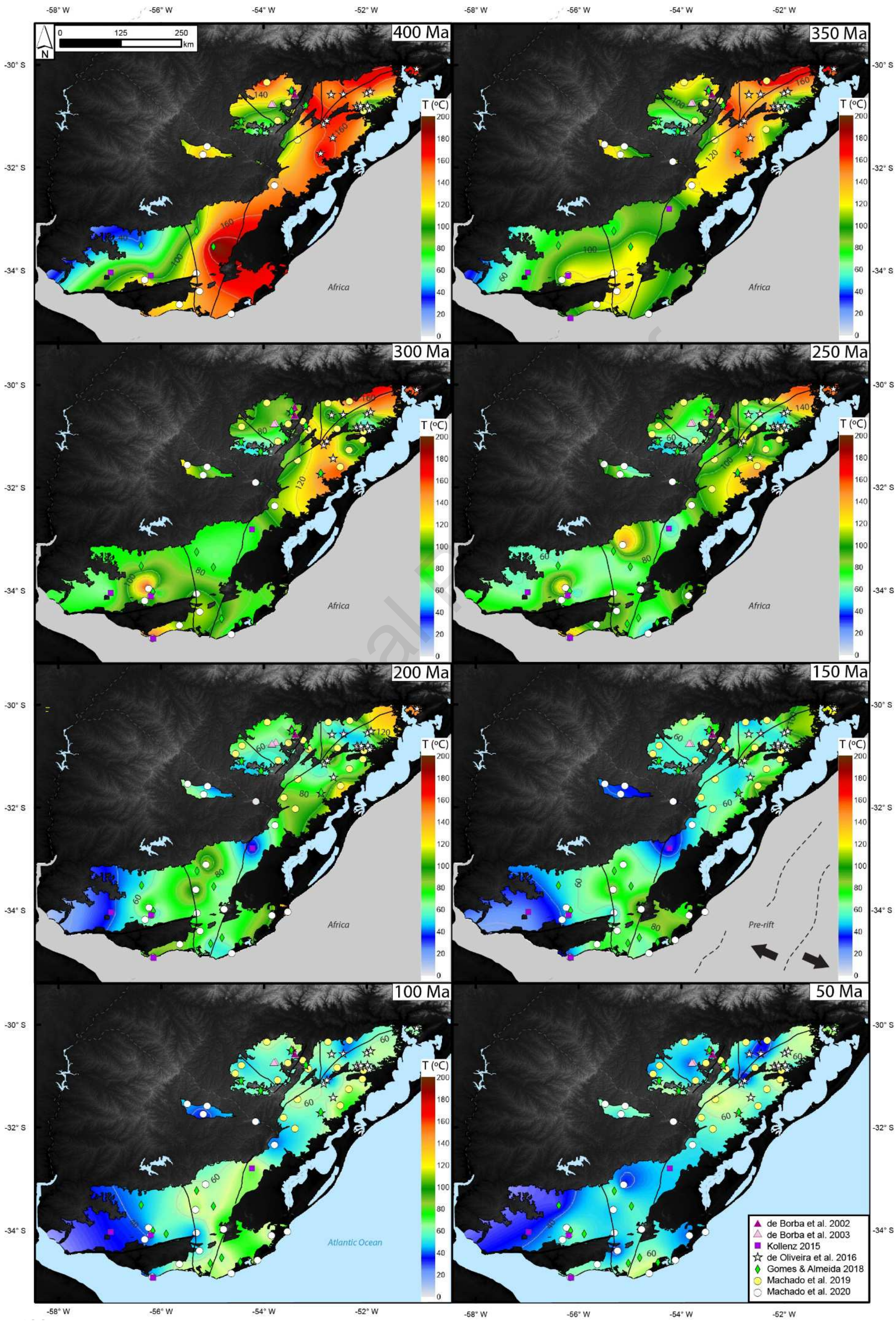
400 Ma
350 Ma
300 Ma
250 Ma
200 Ma
150 Ma
100 Ma
50 Ma
T (°C)
Africa
Pre-rift
Atlantic Ocean
0 125 250 km
N
-58° W
-56° W
-54° W
-52° W
-30° S
-32° S
-34° S
de Borba et al. 2002
de Borba et al. 2003
Kollenz 2015
de Oliveira et al. 2016
Gomes & Almeida 2018
Machado et al. 2019
Machado et al. 2020

Figure 5: Panel with contour maps of the basement temperatures over distinct periods of the Phanerozoic, produced from published AFT-based models. Contour lines represent 20 °C increments. Maps corresponding to older periods have less data for interpolation, as some thermal models used for acquiring the temperatures do not register the sample's temperature too far in past. Note how most of the basement was below 180 °C in the Devonian, and how the Pelotas Batholith took longer to cool down when compared to the rest of the basement. By the Late Jurassic the Nico Pérez and Cuchilla Dionísio terranes appear to have higher temperatures than their surroundings, what could be related to the SaLAM opening and magmatism in the Laguna Merin Basin. Other than that, no significant increase in basement temperature is observed during South Atlantic rifting. FORMAT SUGGESTION: full page.

5 Discussion

In this study we presented the first zircon fission track (ZFT) ages and two new apatite (U-Th)/He ages (AHe) for the Rio de La Plata Craton and the Dom Feliciano Belt, in Uruguay and southern Brazil (Fig. 3). In addition, we integrated these with previously published ages from two other thermochronometers: zircon (U-Th)/He (ZHe) and apatite fission track (AFT) (Fig.6). We also compiled published thermal histories that are based on apatite fission track to extract the temperatures of 77 locations through time, which allowed illustrating the cooling trends modeled for the basement since the Devonian (Fig. 5). The results presented here support a model that both craton and mobile belt have been at temperatures below *c.* 250 °C since the early Paleozoic, and that the basement's cooling to near surface temperatures (T ≤ 60 °C) happened before the breakup of West Gondwana and South Atlantic rifting in the Mesozoic (Fig. 7).

5.1 The early Paleozoic cooling phase

The ZFT ages of the basement reported here range through the entire Paleozoic, with the majority being older than the Silurian. These ages are considerably older than those of de Oliveira et al. (2016) (Fig. 3), who used the ZFT method to date sedimentary rocks from the Camaquã Basin and reported mostly late Paleozoic ages. The difference between the lithologies investigated using the ZFT method does not provide any straightforward explanation of the disagreement between the ages but, as argued by Hueck et al. (2019), zircons from sedimentary rocks present a wider compositional spread, which might bias the ZFT ages due to implicit crystal selection during the analytical procedures. Furthermore, de Oliveira et al. (2016) used the external detector method for the ZFT dating, while we applied the LA-ICP-MS method, which could have had some minor influence in the obtained ages. In any case, the contrasting ages might represent different thermal histories for the Camaquã Basin and the surrounding crystalline basement and demand further studies on the subject.

Similarly, the ZFT ages from the Piedra Alta and Tandilia terranes, southwest of Uruguay, are slightly younger than the rest of the basement (Fig. 3 and 6), which could suggest that part of the Rio de La Plata Craton cooled through temperatures of 240 ± 50 °C only by the middle/late Paleozoic. However, low-eU zircons from the same region resulted in early Paleozoic ZHe ages (Fig. 4), thermochronometer with a lower temperature range (*c.* 190-150 °C), in an apparent contradiction to the ZFT ages. There is no indisputable explanation for such controversy between these ZFT and ZHe ages, but the degree of radiation damage within the crystals might be responsible for the young ZFT ages obtained in the craton. It is argued that the presence of alpha-damage lowers the thermal stability of fission tracks in zircons (Tagami 2005), and that crystals with high levels of accumulated radiation damage appear to have lower ZFT closure temperature (Garver et al. 2005; Marsellos & Garver, 2005). Furthermore, the western samples from the Rio de La Plata Craton, in particular the ones from the Piedra Alta Terrane, present considerable single-crystal ZFT age dispersion, in which low-eU crystals have ages as old as the Mesoproterozoic and high-eU zircons showing ages as young as the Triassic (see Supplementary Material), in a similar way as observed by Garver et al. (2005). Moreover, K-Ar and Ar-Ar ages from the Piedra Alta Terrane indicate cooling through *c*. 420-350 °C during the Paleoproterozoic, without a thermal overprint during the Brasiliano/Pan-African Cycle in the Neoproterozoic-Cambrian (Teixeira et al. 1999; Oyhantçabal et al. 2011). Therefore, the cratonic rocks were maintained at relatively low temperatures (below c. 350 °C) for about 2 Ga, favoring the accumulation of radiation damage within their zircons for a very long time. Thus, we interpret that the somewhat young ZFT ages we obtained in the Piedra Alta and Tandilia terranes reflect a lengthy and slow cooling of the craton, which caused an heterogeneous accumulation of radiation damage within the zircons at relatively low temperatures during many hundreds of millions of years. In consequence, the variable retentivity and stability of fission tracks within each individual zircon led to the dispersed ages, in which highly damaged zircons ultimately resulted in young single-crystal ages. The limited amount of ZFT data prevent further interpretations but raises an exciting opportunity for further studies in the area, such as, for example, whether populations of zircons from a single sample but with different eU content and ages record distinct cooling phases in cratonic regions.

The compilation of ZHe data reinforces the possible control that the zircon eU content exerts in the thermochronometry ages. Both the Rio de La Plata Craton and the Dom Feliciano Belt show a negative correlation between ZHe ages and eU, with low-eU zircons resulting in early Paleozoic ages and high-eU zircons in Mesozoic ages (Fig. 4). The eU control is more evident in the Dom Feliciano Belt, the zircons of which presents a wider range of eU content (Fig. 4B2'). This is a well-known negative correlation in ZHe ages (e.g. Reiners, 2005; Guenthner et al. 2013), and makes evident how ZHe analysis can be biased because of crystal selection. It is recommended, during ZHe dating, to analyze zircons with variable levels of opacity, which is a proxy for the level of the crystal metamictization, thus allowing evaluation of the influence of eU in the obtained ages (Ault et al. 2018).

In any case, the general concordance between ZFT and ZHe ages, especially among those zircons less affected by the radiation damage, suggests a fast cooling of the basement from *c.* 290 to 150 °C during the early Paleozoic, corresponding to the temperature interval covered by these thermochronometers. Such a cooling phase likely represents a stage of thermal relaxation and general exhumation of the basement after the end of the Brasiliano/Pan-African Cycle (Neoproterozoic to Cambrian) (Fig. 7). Furthermore, K-Ar ages from shear zones and faults corroborate tectonic activity in Uruguay between the Cambrian and Devonian (Hueck et al. 2017).

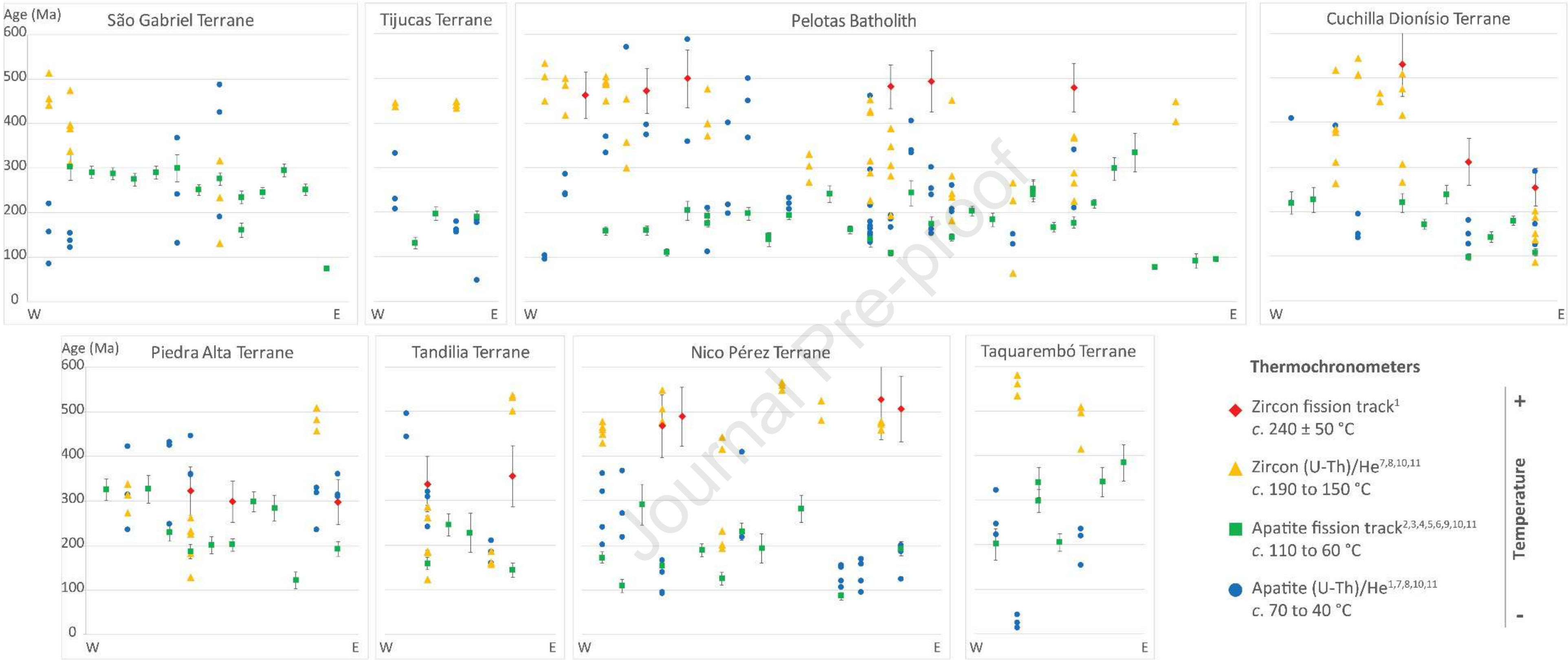

Figure 6: Compilation of zircon fission track and (U-Th)/He ages, and of apatite fission track and (U-Th)/He ages published in the region. Ft corrected (U-Th/He) ages and fission track central ages are reported, with 1σ error bars. The top panel shows ages for the Dom Feliciano Belt and the bottom ages for the Rio de La Plata Craton. Terranes and ages are organized from west to east according to samples longitude, but not to scale. Ages vertically aligned were obtained at the same location. Ages are from 1) This work; 2) Bicca et al. 2013; 3) de Borba et al. 2002; 4) de Borba et al. 2003; 5) de Oliveira et al. 2016; 6) Gomes & Almeida, 2019; 7) Hueck et al. 2017; 8) Hueck et al. 2019; 9) Kollenz 2015; 10) Machado et al. 2019; and 11) Machado et al. 2020. FORMAT SUGGESTION: Sideways, 1.5 column wide or full page.

5.2 The West Gondwana breakup event

The integration of the thermochronometry data from the Rio de La Plata Craton and Dom Feliciano Belt suggests that both units went through very similar thermal histories through the Phanerozoic. Based on the results of the ZFT and ZHe thermochronometers from this work, Hueck et al. (2017, 2019) and Machado et al. (2019, 2020), it seems that most of the region went through a cooling/exhumation phase in the early Paleozoic, after the end of the Brasiliano/Pan-African Cycle, and reached temperatures below 200 °C before the Devonian. However, the thermal history for the Rio de La Plata Craton and Dom Feliciano Belt after this initial cooling phase is still a matter of debate.

Thermal models based only in (U-Th)/He data from Hueck et al. (2017, 2019) support either (1) an hypothesis in which samples were near the surface ($T \leq 60$ °C) by the Silurian but could be reheated to temperatures up to 100 °C after that, or (2) a hypothesis without the low temperatures ($T \leq 60$ °C) in the Silurian, in which samples remained at temperatures higher than 60 °C until the Triassic. The authors argue in favor of the first scenario, claiming that the basement reached near surface temperatures during the Silurian and then went through cycles of burial and exhumation correlated to the Paraná Basin depositional cycles. As mentioned in section 4.2, such a long period at low temperatures and the successive cycles of reheating due to sedimentation and erosion could explain the dispersion of the AHe ages. Moreover, it is likely that sediments from the Paraná Basin had covered, at least partially, the present-day exposed crystalline rocks (Fig. 7), as a basement window of the Nico Pérez Terrane crops out of the Paraná Basin in the north of Uruguay (Isla Cristalina de Rivera) (Fig. 2), and minor remnants of the Gondwana II supersequence from the Paraná Basin are present over the Dom Feliciano Belt in Brazil.

On the other hand, the AFT data and models from de Borba et al. (2002, 2003), Kollenz (2015), de Oliveira et al. (2016), Gomes & Almeida (2019) and Machado et al. (2019, 2020) suggest, for most of the basement, temperatures above 120 °C in the Early Devonian (400 Ma), and around 100 °C in the Carboniferous-Permian transition (300 Ma) (Fig. 5). The cooling trend observed in Figure 5 is interpreted as a representation of the basement exhumation, which progressively brought deeply buried rocks to shallower and cooler regions of the crust. Furthermore, the 97 AFT ages compiled from published studies range from 383 ± 40 Ma to 74 ± 5Ma, of which 74 ages are Mesozoic, mostly Jurassic (Figs. 3 and 6). This large dataset AFT data and models indicate that the Rio de La Plata Craton and Dom Feliciano Belt cooled down between *c.* 110° and 60 °C only in the Mesozoic, before the West Gondwana breakup, hence exposure to near surface conditions ($T \leq 60$ °C) in the Silurian is less likely. This does not rule out the hypothesis of partial burial of the region by the cycles of the Paraná Basin, whereas maturation studies on the basin suggest that the sedimentary packages did not exceed 100 °C since the Devonian (da Silva & Cornford, 1985; Machado et al. 2020).

According to the compilation of AFT models from the aforementioned authors (Fig. 5), most of the Rio de La Plata Craton and Dom Feliciano Belt reached temperatures near or below 60 °C by the Jurassic, before the Paraná-Etendeka LIP event and the South Atlantic opening. Temperatures would then have remained around 60 °C until at least the end of Mesozoic, with some locations passing through a subtle reheating immediately after the breakup, as observed in models from Kollenz (2015), de Oliveira et al. (2016) and Machado et al. (2019, 2020). Therefore, this reheating could have caused the dispersion of the AHe ages obtained in the region (Fig. 4). Such a reheating phase is backed up by the geological evidence of voluminous magmatism associated with the South Atlantic opening: Permo-Triassic to late Cretaceous alkaline magmatism is recorded in the margins of the Paraná Basin (Riccomini et al. 2005), the Paraná-Etendeka LIP surrounded the craton and belt *c.* 134 Ma ago (Turner et al. 1994; Rosseti et al. 2014), dikes swarms associated with the Paraná-Etendeka LIP were recently identified in South Brazil and Uruguay (Hartmann et al. 2016; Demarco et al. 2020), the forming marginal Pelotas Basin records intense magmatism during its early development (Beglinger et al. 2012; Stica et al. 2014; McDermott et al. 2019), the Laguna Merin Basin in Uruguay was filled with volcanic rocks *c.* 130 Ma ago (Cernuschi et al. 2015), and alkaline magmatism is recorded in the study region until the late Cretaceous (Barbieri et al. 1987; Gaucher et al. 2016). Furthermore, the West Gondwana breakup and LIP event are often related to the presence of the Tristan da Cunha mantle plume, the thermal influence area of which includes the craton and belt, and is recorded on the oceanic plates following breakup (White & McKenzie, 1989; Turner et al. 1994; Meisling et al. 2001; Gibson et al. 2006). The sum of all these volcanic events likely increased the regional geotherm gradient during the Cretaceous. In addition, the Mesozoic cooling/exhumation of the region could have been caused by mantle plume push and magma accumulation beneath the lithosphere before breakup, which would increase the stretched continental plate buoyancy and cause elevated topography during rifting (White & McKenzie, 1989; Quirk & Rüpke 2018; Machado et al. 2019, 2020). Hence, the hypothesis of a protracted cooling of the Rio de La Plata Craton and the Dom Feliciano Belt during the Paleozoic and Mesozoic is feasible, with the basement reaching temperatures near 60 °C just before South Atlantic opening, and going through a thermal disturbance with subtle reheating caused by the various magmatic events during the Cretaceous. This thermal history better fits the AFT models from de Borba et al. (2002, 2003), Kollenz (2015), de Oliveira et al. (2016), Gomes &

Almeida (2019) and Machado et al. (2019, 2020), incorporates the trend of younger AFT ages towards the volcanic margin northeast, and the AHe age dispersion as well.

Independently of the thermal history and exhumation path during the Paleozoic and Mesozoic, there is general agreement that the basement was near the surface ($T \leq 60$ °C) before the West Gondwana breakup, and that exhumation after the rift was minor (Fig. 7). The topography profile, with peaks under 500 m on the Rio de La Plata Craton and Dom Feliciano Belt, also suggests a period of minimum vertical movements of the crust, with predominance of weathering and erosion after breakup. This contrasts with the thermotectonic behavior of the South America passive margin northwards, which presents higher topography, with peaks over 2.000 m, and significant syn and post-rift exhumation (e.g. Gallagher *et al.* 1994, 1995; Saenz *et al.* 2003; Hackspacher *et al.* 2004; Hiruma *et al.* 2010; Cogné *et al.* 2011, 2012; Karl *et al.* 2013). The transition between these distinct crustal behaviors appears to be near the city of Florianópolis, approximately in the limit between the Pelotas and Santos basins, and the low continental topography to the south and the higher to the north (Figs. 1 and 2). This region is also connected to the mid-ocean ridge through the Rio Grande Fracture Zone (a.k.a. Florianópolis Fracture Zone), one of the most prominent transfer zones in the oceanic crust and which had an important role during the South Atlantic opening and plate rotation (Torsvik et al. 2009; Stica et al. 2014; Granot & Dyment 2015; Graça et al. 2019).

In any case, it appears that the key to constraining the recent thermotectonic history of the Rio de La Plata Craton and Dom Feliciano Belt is to better comprehend what information the AHe age dispersion possesses. This thermochronometer has the potential to define when and for how long the basement in the region sustained near-surface temperatures, and how effective were the reheating phases caused by burial under the Paraná Basin sediments and by the magmatism during the West Gondwana breakup. There are still unknowns about the (U-Th)/He system that should be addressed to allow more reliable thermal histories to be derived solely from it (Green & Duddy 2018), especially in a region like this, where the accumulation of radiation damage within apatites and zircons appears to play a major role in the thermochronometry ages.

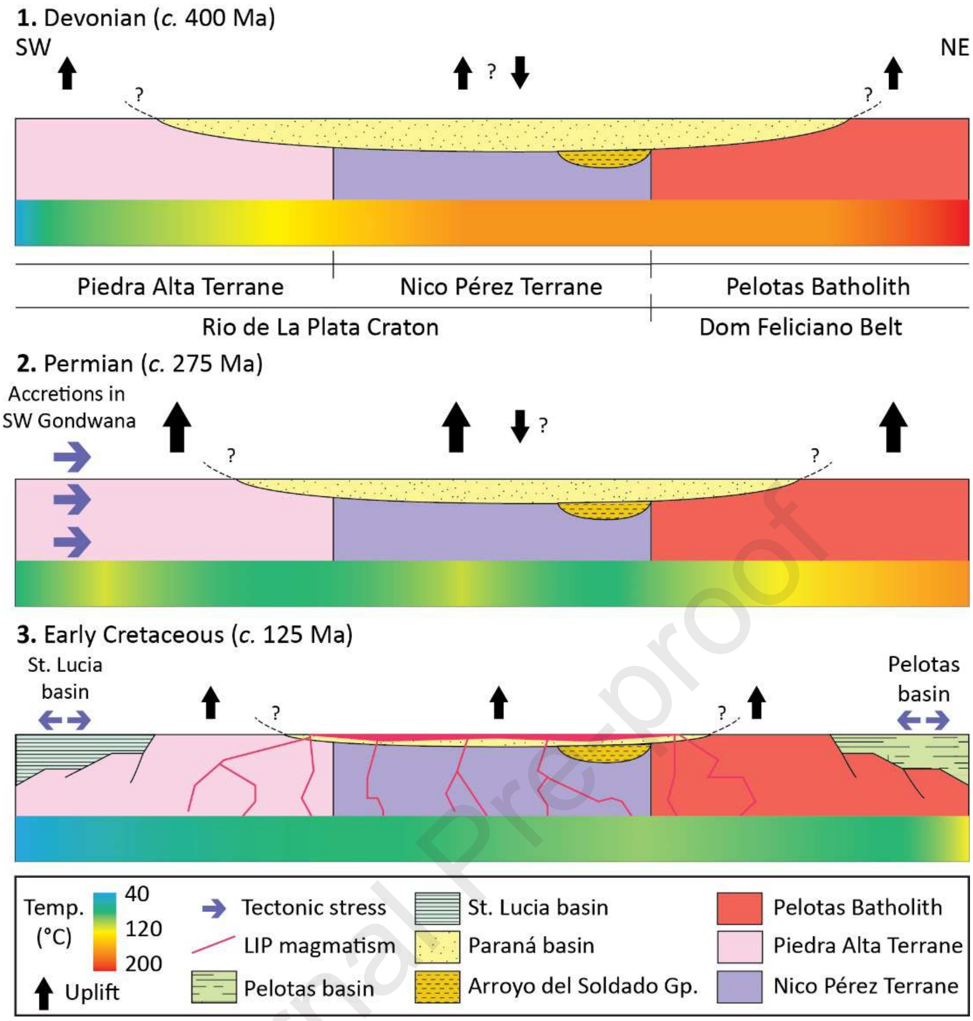

Figure 7: Schematic cross section along the Rio de La Plata Craton and Dom Feliciano Belt, as shown in Figure 2, and with basement temperatures from Figure 5. Question marks indicate uncertainty in the extent of the Paraná Basin. 1) General post-Brasiliano/Pan-African basement exhumation, suggested by zircon thermochronometry and AFT inverse models, with uncertainty about the subsidence and area covered by the Paraná Basin (Paraná supersequence). At the time, temperatures in the Piedra Alta Terrane were considerably lower than in the Pelotas Batholith. 2) Beginning of the period of more intense regional uplift, which lasted until middle Mesozoic, suggested by AFT ages and inverse models. Such a phase is likely related to the far-field propagation of tectonic stress caused by plate collision and accretionary processes on the SW margin of West Gondwana, and subsequently by mantle push and lithospheric thinning before the South Atlantic opening (Jurassic-Cretaceous). Local subsidence and sedimentation of the Paraná Basin (Gondwana I and II supersequences) might have happened at the same time of regional uplift. The Pelotas Batholith maintained its higher temperatures relative to the rest of the region, and local high temperatures were observed in some published thermal models. 3) During the West Gondwana breakup and South Atlantic opening, the rocks exposed at present were already near the surface (temperatures near 60 °C). All magmatism associated with the breakup event was not enough to reset any of the low-temperature thermochronometers, but maintained the basement temperatures near 60-70 °C for a long time, favoring the overdispersion of AHe ages. FORMAT SUGGESTION: 1.5 or 2 column wide.

6 Conclusions

In this study we have provided the first ZFT ages for the Rio de La Plata Craton and Dom Feliciano Belt, on the passive margin of South America. We also reviewed the previously published data from apatite fission tracks and apatite and zircon (U-Th)/He, plus the thermal histories modeled for the region. The current thermochronology dataset of the region encompasses 26 ZFT ages, 139 single crystal ZHe ages, 97 AFT ages and 131 single crystal AHe ages, plus 77 inverse thermal models based on AFT data. This large dataset indicates a protracted and complex thermal history for the crystalline basement, of which some questions remain open for further investigation.

The thermal history of both craton and belt includes an early Paleozoic cooling phase, suggested by the ZFT and ZHe data, in which the basement reached temperatures below *c.* 200 °C. Such a cooling phase is likely related to regional exhumation after the end of the Brasiliano/Pan-African Cycle (Neoproterozoic-Cambrian) and formation of West Gondwana. After this initial cooling, the thermal history is still open to discussion. While some studies suggest that most of the basement reached temperatures below 60 °C in the Silurian (Hueck et al. 2017, 2019), others support a model where these temperatures were reached only in the Paleozoic-Mesozoic transition (this work; de Borba et al. 2002, 2003; de Oliveira et al. 2016; Gomes & Almeida 2019; Machado et al. 2019, 2020). In any case, it is likely the Paraná Basin sedimentary cycles were responsible for partial burial of the crystalline basement during the Paleozoic, which might have caused a minor increase in the basement temperatures. Besides, the magmatism associated with the South Atlantic opening probably caused a temperature disturbance in the region during the Cretaceous, maintaining the basement near 60 °C for 100 Ma or even increasing the temperature at some locations, as indicated by models from Kollenz (2015), de Oliveira et al. (2016), Gomes & Almeida (2019) and Machado et al. (2019, 2020). The observed AHe age dispersion supports a subtle reheating of the basement during the Phanerozoic, but the mechanism driving such a temperature increase is not clear yet. During the breakup, the rocks exposed at present in the Rio de La Plata Craton and Dom Feliciano Belt were already near the surface ($T \leq 60$ °C). After the rift, cooling and exhumation were minor in the region, in contrast to the South Atlantic margin to the north.

The dispersion of the AHe ages appears to contain the key to a fuller understanding of the final cooling/exhumation paths of the Rio de La Plata Craton and Dom Feliciano Belt in the Phanerozoic. Further studies of the behavior of this thermochronometer, the influence of eU content and radiation damage within apatites and zircons during long periods at low temperatures, and the effects of minor reheating phases in age dispersion are recommended to better constrain the thermal history of the region and other areas with comparable geological contexts.

7 Acknowledgments

The authors gratefully acknowledge the support from Shell Brasil through the "BG05: UoA-UFRGS-SWB Sedimentary Systems" project at UFRGS and UoA, and the strategic importance of the support given by ANP through the R&D levy regulation. J.P. Machado thanks the CNPq (SWE 204254/2017-5) for the exchange period at the University of Aberdeen, and A.R. Jelinek also thanks the support from CNPq (Project 303184/2017-5). We are grateful for the helpful and constructive reviews from Mathias Hueck, Mauricio Parra and an anonymous reviewer, that greatly improved this manuscript.

8 References

Amante, C., & Eakins, B. W. (2009). ETOPO1 1 Arc-minute global relief model: procedures, data sources and analysis. NOAA Technical Memorandum NESDIS NGDC-24. *National Geophysical Data Center, NOAA*, *10*, V5C8276M.

Aslanian, D., Moulin, M., Olivet, J. L., Unternehr, P., Matias, L., Bache, F., ... & Labails, C. (2009). Brazilian and African passive margins of the Central Segment of the South Atlantic Ocean: Kinematic constraints. *Tectonophysics*, *468*(1-4), 98-112.

Ault, A. K., Guenthner, W. R., Moser, A. C., Miller, G. H., & Refsnider, K. A. (2018). Zircon grain selection reveals (de) coupled metamictization, radiation damage, and He diffusivity. Chemical Geology, 490, 1-12.

Barbieri, M., Beccaluva, L., Brotzu, P., Conte, A., Garbarino, C., Gomes, C. B., ... & Tamura, R. M. (1987). Petrological and geochemical studies of alkaline rocks from continental Brazil. 1. The phonolite suite from Piratini, RS. *Geochimica Brasiliensis*, *1*(1), 109-138.

Basei, M. A. S., Frimmel, H. E., Nutman, A. P., Preciozzi, F., & Jacob, J. (2005). A connection between the Neoproterozoic Dom Feliciano (Brazil/Uruguay) and Gariep (Namibia/South Africa) orogenic belts–evidence from a reconnaissance provenance study. *Precambrian Research*, *139*(3-4), 195-221.

Basei, M. A., Peel, E., Bettucci, L. S., Preciozzi, F., & Nutman, A. P. (2011). The basement of the Punta del Este Terrane (Uruguay): an African Mesoproterozoic fragment at the eastern border of the South American Río de La Plata craton. *International Journal of Earth Sciences*, *100*(2-3), 289-304.

Beglinger, S. E., Doust, H., & Cloetingh, S. (2012). Relating petroleum system and play development to basin evolution: Brazilian South Atlantic margin. *Petroleum Geoscience*, *18*(3), 315-336.

Bernet, M., & Garver, J. I. (2005). Fission-track analysis of detrital zircon. *Reviews in Mineralogy and Geochemistry*, *58*(1), 205-237.

Bernet, M., Brandon, M. T., Garver, J. I., & Molitor, B. R. (2004). Fundamentals of detrital zircon fission-track analysis for provenance and exhumation studies with examples from the European Alps. *Special Papers-Geological Society Of America*, 25-36.

Bertolini, G., Marques, J., Hartley, A.J., DaRosa, A.A., S. Scherer, C.M., Basei, M.A. and Frantz, J.C., (2020). Controls on Early Cretaceous desert sediment provenance in south-west Gondwana, Botucatu Formation (Brazil and Uruguay). *Sedimentology*.

Bicca, M. M., Chemale Jr, F., Jelinek, A. R., de Oliveira, C. H. E., Guadagnin, F., & Armstrong, R. (2013). Tectonic evolution and provenance of the Santa Bárbara Group, Camaquã Mines region, Rio Grande do Sul, Brazil. *Journal of South American Earth Sciences*, *48*, 173-192.

Blanco, G., Rajesh, H.M., Gaucher, C., Germs, G.J.B. & Chemale, F. (2009). Provenance of the Arroyo del Soldado Group (Ediacaran to Cambrian, Uruguay): Implications for the paleogeographic evolution of southwestern Gondwana. *Precambrian Research*, 171, 57–73.

Bossi, J., & Gaucher, C. (2004). The Cuchilla Dionisio Terrane, Uruguay: an allochthonous block accreted in the Cambrian to SW-Gondwana. *Gondwana Research*, *7*(3), 661-674.

Bossi, J., & Cingolani, C. (2009). Extension and general evolution of the Río de la Plata Craton. *Developments in Precambrian Geology*, *16*, 73-85.

Brown, R. W., Gallagher, K., Gleadow, A. J., & Summerfield, M. A. (2000). Morphotectonic evolution of the South Atlantic margins of Africa and South America. *Geomorphology and global tectonics*, 255-281.

Brown, R. W., Beucher, R., Roper, S., Persano, C., Stuart, F., & Fitzgerald, P. (2013). Natural age dispersion arising from the analysis of broken crystals. Part I: Theoretical basis and implications for the apatite (U–Th)/He thermochronometer. *Geochimica et Cosmochimica Acta*, *122*, 478-497.

Bueno, G. V., Zacharias, A. A., Oreiro, S. G., Cupertino, J. A., Falkenhein, F. U. H., & Neto, M. M. (2007). Bacia de Pelotas. *Boletim de Geociencias da Petrobras*, *15*(2), 551-559.

Buiter, S. J., & Torsvik, T. H. (2014). A review of Wilson Cycle plate margins: A role for mantle plumes in continental break-up along sutures?. *Gondwana Research*, *26*(2), 627-653.

Ceolin, D., Fauth, G., & Coimbra, J. C. (2011). Cretaceous–Lower Paleogene ostracods from the Pelotas Basin, Brazil. *Palaeobiodiversity and Palaeoenvironments*, *91*(2), 111-128.

Cernuschi, F., Dilles, J. H., Kent, A. J. R., Schroer, G., Raab, A. K., Conti, B., & Muzio, R. (2015). Geology, geochemistry and geochronology of the Cretaceous Lascano East Intrusive Complex and magmatic evolution of the Laguna Merin Basin, Uruguay. *Gondwana Research*, *28*(2), 837-857.

Chang, H. K., Kowsmann, R. O., Figueiredo, A. M. F., & Bender, A. (1992). Tectonics and stratigraphy of the East Brazil Rift system: an overview. *Tectonophysics*, *213*(1-2), 97-138.

Chemale Jr, F. (2000). Evolução geológica do Escudo Sul-rio-grandense. *Geologia do Rio Grande do Sul*. Porto Alegre, CIGO-UFRGS, 13-52.

Cogné, N., Gallagher, K., & Cobbold, P. R. (2011). Post-rift reactivation of the onshore margin of southeast Brazil: evidence from apatite (U–Th)/He and fission-track data. *Earth and Planetary Science Letters*, *309*(1-2), 118-130.

Cogné, N., Gallagher, K., Cobbold, P. R., Riccomini, C., & Gautheron, C. (2012). Post-breakup tectonics in southeast Brazil from thermochronological data and combined inverse-forward thermal history modeling. *Journal of Geophysical Research: Solid Earth*, *117*(B11).

Cogné, N., Chew, D. M., Donelick, R. A., & Ansberque, C. (2020). LA-ICP-MS apatite fission track dating: A practical zeta-based approach. Chemical Geology, 531, 119302.

Cordani, U. G., Melcher, G. C., & Almeida, F. D. (1968). Outline of the Precambrian geochronology of South America. *Canadian Journal of Earth Sciences*, *5*(3), 629-632.

da Silva, Z. C. C., & Cornford, C. (1985). The kerogen type, depositional environment and maturity, of the Irati Shale, Upper Permian of Paraná Basin, Southern Brazil. *Organic geochemistry*, *8*(6), 399-411.

de Almeida, F. F. M., Hasui, Y., de Brito Neves, B. B., & Fuck, R. A. (1981). Brazilian structural provinces: an introduction. *Earth-Science Reviews*, *17*(1-2), 1-29.

de Borba, A. W., Vignol-Lelarge, M. L. M., & Mizusaki, A. M. P. (2002). Uplift and denudation of the Caçapava do Sul granitoids (southern Brazil) during Late Paleozoic and Mesozoic: constraints from apatite fission-track data. *Journal of South American Earth Sciences*, *15*(6), 683-692.

de Borba, A. W., de Lima, E. F., Vignol-Lelarge, M. L. M., Mizusaki, A. M. P., Sparrenberg, I., & de Barros, C. E. (2003). Significance of Late Paleozoic fission-track ages in volcanic rocks from the Lavras do Sul region, southernmost Brazil. *Gondwana Research*, *6*(1), 79-88.

de Brito Neves, B. B., & Fuck, R. A. (2013). Neoproterozoic evolution of the basement of the South-American platform. *Journal of South American Earth Sciences*, *47*, 72-89.

de Brito Neves, B. B., Fuck, R. A., & Pimentel, M. M. (2014). The Brasiliano collage in South America: a review. *Brazilian Journal of Geology*, *44*(3), 493-518.

de Oliveira, C.H.E., Chemale, F., Jelinek, A.R., Bicca, M.M. & Philipp, R.P. (2014). U–Pb and Lu–Hf isotopes applied to the evolution of the late to postorogenic transtensional basins of the Dom Feliciano belt, Brazil. *Precambrian Research*, 246, 240–255,

de Oliveira, C. H. E., Jelinek, A. R., Chemale Jr, F., & Bernet, M. (2016). Evidence of post-Gondwana breakup in Southern Brazilian Shield: Insights from apatite and zircon fission track thermochronology. *Tectonophysics*, *666*, 173-187.

Demarco, P. N., Masquelin, H., Prezzi, C., Aifa, T., Muzio, R., Loureiro, J., ... & Bettucci, L. S. (2020). Aeromagnetic patterns in Southern Uruguay: Precambrian-Mesozoic dyke swarms and Mesozoic rifting structural and tectonic evolution. Tectonophysics, 228373.

Dias, J. L., Sad, A. R., Fontana, R. L., & Feijó, F. J. (1994). Bacia de Pelotas. *Boletim de Geociencias da Petrobras*, *8*(1), 235-245.

Donelick, R.A, O'Sullivan, P.B., and Ketcham, R.A. 2005. Apatite fission-track analysis. Reviews in Mineralogy and Geochemistry, 58: 49–94.

Farley, K. A., Wolf, R. A., & Silver, L. T. (1996). The effects of long alpha-stopping distances on (U-Th)/He ages. *Geochimica et cosmochimica acta*, *60*(21), 4223-4229.

Flowers, R. M. (2009). Exploiting radiation damage control on apatite (U–Th)/He dates in cratonic regions. *Earth and Planetary Science Letters*, *277*(1-2), 148-155.

Flowers, R. M., Shuster, D. L., Wernicke, B. P., & Farley, K. A. (2007). Radiation damage control on apatite (U-Th)/He dates from the Grand Canyon region, Colorado Plateau. *Geology*, *35*(5), 447-450.

Fox, M., & Shuster, D. L. (2014). The influence of burial heating on the (U–Th)/He system in apatite: Grand Canyon case study. *Earth and Planetary Science Letters*, *397*, 174-183.

Gallagher, K., Hawkesworth, C. J., & Mantovani, M. S. M. (1994). The denudation history of the onshore continental margin of SE Brazil inferred from apatite fission track data. *Journal of Geophysical Research: Solid Earth*, *99*(B9), 18117-18145.

Gallagher, K., Hawkesworth, C. J., & Mantovani, M. S. M. (1995). Denudation, fission track analysis and the long-term evolution of passive margin topography: application to the southeast Brazilian margin. *Journal of South American Earth Sciences*, *8*(1), 65-77.

Garver, J. I., Reiners, P. W., Walker, L. J., Ramage, J. M., & Perry, S. E. (2005). Implications for timing of Andean uplift from thermal resetting of radiation-damaged zircon in the Cordillera Huayhuash, northern Peru. The Journal of Geology, 113(2), 117-138.

Gaucher, C., Finney, S. C., Poiré, D. G., Valencia, V. A., Grove, M., Blanco, G., ... & Peral, L. G. (2008). Detrital zircon ages of Neoproterozoic sedimentary successions in Uruguay and Argentina: insights into the geological evolution of the Río de la Plata Craton. *Precambrian Research*, *167*(1-2), 150-170.

Gaucher, C., Frei, R., Chemale, F., Frei, D., Bossi, J., Martínez, G., ... & Cernuschi, F. (2011). Mesoproterozoic evolution of the Río de la Plata Craton in Uruguay: at the heart of Rodinia?. *International Journal of Earth Sciences*, *100*(2-3), 273-288.

Gaucher, C., Babinski, M., Blanco, G. (2016). Riolitas del Cretácico Superior (Campaniense); el magmatismo más joven de Uruguay. In: *VIII Congreso Uruguayo de Geología, Actas*, pp. 160-161, Montevideo.

Gibson, S. A., Thompson, R. N., & Day, J. A. (2006). Timescales and mechanisms of plume–lithosphere interactions: 40Ar/39Ar geochronology and geochemistry of alkaline igneous rocks from the Paraná–Etendeka large igneous province. *Earth and Planetary Science Letters*, *251*(1-2), 1-17.

Gladczenko, T. P., Hinz, K., Eldholm, O., Meyer, H., Neben, S., & Skogseid, J. (1997). South Atlantic volcanic margins. *Journal of the Geological Society*, *154*(3), 465-470.

Gleadow, A. J. W., Duddy, I. R., Green, P. F., & Lovering, J. F. (1986). Confined fission track lengths in apatite: a diagnostic tool for thermal history analysis. *Contributions to Mineralogy and Petrology*, *94*(4), 405-415.

Gomes, C. H., & Almeida, D. (2019). New insights into the Gondwana breakup at the Southern South America by apatite fission-track analyses. *Advances in Geosciences*, *47*, 1-15.

Graça, M. C., Kusznir, N., & Stanton, N. S. G. (2019). Crustal thickness mapping of the central South Atlantic and the geodynamic development of the Rio Grande Rise and Walvis Ridge. *Marine and Petroleum Geology*, *101*, 230-242.

Granot, R., & Dyment, J. (2015). The cretaceous opening of the South Atlantic Ocean. *Earth and Planetary Science Letters*, *414*, 156-163.

Green, P. F., & Duddy, I. R. (2006). Interpretation of apatite (U–Th)/He ages and fission track ages from cratons. *Earth and Planetary Science Letters*, *244*(3-4), 541-547.

Green, P., & Duddy, I. (2018). Apatite (U-Th-Sm)/He thermochronology on the wrong side of the tracks. *Chemical Geology*, *488*, 21-33.

Guenthner, W. R., Reiners, P. W., Ketcham, R. A., Nasdala, L., & Giester, G. (2013). Helium diffusion in natural zircon: Radiation damage, anisotropy, and the interpretation of zircon (U-Th)/He thermochronology. *American Journal of Science*, *313*(3), 145-198.

Hackspacher, P. C., Ribeiro, L. F. B., Ribeiro, M. C. S., Fetter, A. H., Neto, J. H., Tello, C. E. S., & Dantas, E. L. (2004). Consolidation and break-up of the South American platform in southeastern Brazil: tectonothermal and denudation histories. *Gondwana Research*, *7*(1), 91-101.

Hartmann, L. A., Campal, N., Santos, J. O. S., McNaughton, N. J., Bossi, J., Schipilov, A., & Lafon, J. M. (2001). Archean crust in the Rio de la Plata Craton, Uruguay—SHRIMP U–Pb zircon reconnaissance geochronology. *Journal of South American Earth Sciences*, *14*(6), 557-570.

Hartmann, L. A., Santos, J. O. S., Cingolani, C. A., & McNaughton, N. J. (2002). Two Paleoproterozoic orogenies in the evolution of the Tandilia Belt, Buenos Aires, as evidenced by zircon U-Pb SHRIMP geochronology. *International Geology Review*, *44*(6), 528-543.

Hartmann, L. A., Chemale Jr, F., & Philipp, R. P. (2007). Evolução geotectônica do Rio Grande do Sul no pré-cambriano. *Ianuzzi R. & Frantz JC.(Org.)*, *50*, 97-123.

Hartmann, L. A., Lopes, W. R., & Savian, J. F. (2016). Integrated evaluation of the geology, aerogammaspectrometry and aeromagnetometry of the Sul-Riograndense Shield, southernmost Brazil. *Anais da Academia Brasileira de Ciências*, *88*(1), 75-92.

Hasebe, N., Barbarand, J., Jarvis, K., Carter, A., and Hurford, A.J. 2004. Apatite fission-track chronometry using laser ablation ICP-MS. Chemical Geology, 207: 135–145

Hasebe, N., Tamura, A., & Arai, S. (2013). Zeta equivalent fission-track dating using LA-ICP-MS and examples with simultaneous U–P b dating. *Island Arc*, *22*(3), 280-291.

Hasui, Y. (2010). A grande colisão pré-cambriana do sudeste brasileiro e a estruturação regional. *Geociências*, 141-169.

Hiruma, S. T., Riccomini, C., Modenesi-Gauttieri, M. C., Hackspacher, P. C., Neto, J. C. H., & Franco-Magalhães, A. O. (2010). Denudation history of the Bocaina Plateau, Serra do Mar, southeastern Brazil: Relationships to Gondwana breakup and passive margin development. *Gondwana Research*, *18*(4), 674-687.

Hueck, M., Oriolo, S., Dunkl, I., Wemmer, K., Oyhantçabal, P., Schanofski, M., ... & Siegesmund, S. (2017). Phanerozoic low-temperature evolution of the Uruguayan Shield along the South American passive margin. *Journal of the Geological Society*, *174*(4), 609-626.

Hueck, M., Dunkl, I., Oriolo, S., Wemmer, K., Basei, M. A., & Siegesmund, S. (2019). Comparing contiguous high-and low-elevation continental margins: New (U-Th)/He constraints from South Brazil and an integration of the thermochronological record of the southeastern passive margin of South America. *Tectonophysics*, *770*, 228222.

Hurford, A. J. (1986). Cooling and uplift patterns in the Lepontine Alps South Central Switzerland and an age of vertical movement on the Insubric fault line. *Contributions to mineralogy and petrology*, *92*(4), 413-427.

Jelinek, A. R., Neto, A. C. B., & Poupeau, G. (2016). Análise por traços de fissão em apatitas do distrito fluorítico de Santa Catarina: relações entre hidrotermalismo e evolução da margem continental. *Revista Brasileira de Geociências*, *33*(3), 289-298.

Karl, M., Glasmacher, U. A., Kollenz, S., Franco-Magalhaes, A. O., Stockli, D. F., & Hackspacher, P. C. (2013). Evolution of the South Atlantic passive continental margin in southern Brazil derived from zircon and apatite (U–Th–Sm)/He and fission-track data. *Tectonophysics*, *604*, 224-244.

Kasanzu, C. H. (2017). Apatite fission track and (U-Th)/He thermochronology from the Archean Tanzania Craton: Contributions to cooling histories of Tanzanian basement rocks. *Geoscience Frontiers*, *8*(5), 999-1007.

Kollenz, S. (2015). *Long-term landscape evolution, cooling and exhumation history of the South American passive continental margin in NE Argentina & SW Uruguay* (Doctoral dissertation - Heidelberg Univeristy).

Košler, J., & Sylvester, P. J. (2003). Present trends and the future of zircon in geochronology: laser ablation ICPMS. *Reviews in mineralogy and geochemistry*, *53*(1), 243-275.

Machado, J. P. S., Jelinek, A. R., Bicca, M. M., Stephenson, R., & Genezini, F. A. (2019). West Gondwana orogenies and Pangaea break-up: thermotectonic effects on the southernmost Mantiqueira Province, Brazil. *Journal of the Geological Society*, *176*(6), 1056-1075.

Machado, J. P. S. L., Jelinek, A. R., Stephenson, R., Gaucher, C., Bicca, M. M., Chiglino, L., & Genezini, F. A. (2020). Low-temperature thermochronology of the South Atlantic margin along Uruguay and its relation to tectonic events in West Gondwana. *Tectonophysics*, 228439.

Maraschin, A.J., Mizusaki, A.M., Zwingmann, H., de Borba, A.W. & Sbrissa, G.F. (2010). Illite authigenesis in sandstones of the Guaritas Allogroup (Early Paleozoic): Implications for the depositional age, stratigraphy and evolution of the Camaquã Basin (Southern Brazil). *Journal of South American Earth Sciences*, 29, 400–411

Marsellos, A. E., & Garver, J. I. (2010). Radiation damage and uranium concentration in zircon as assessed by Raman spectroscopy and neutron irradiation. *American Mineralogist*, *95*(8-9), 1192-1201.

McDermott, C., Collier, J. S., Lonergan, L., Fruehn, J., & Bellingham, P. (2019). Seismic velocity structure of seaward-dipping reflectors on the South American continental margin. *Earth and Planetary Science Letters*, *521*, 14-24.

Meisling, K. E., Cobbold, P. R., & Mount, V. S. (2001). Segmentation of an obliquely rifted margin, Campos and Santos basins, southeastern Brazil. *AAPG bulletin*, *85*(11), 1903-1924.

Milani, E. J. (1997). *Evolução tectono-estratigráfica da Bacia do Paraná e seu relacionamento com a geodinâmica fanerozóica do Gondwana sul-ocidental* (Doctoral dissertation, Universidade Federal do Rio Grande do Sul.).

Milani, E. J., & Ramos, V. A. (1998). Orogenias paleozóicas no domínio sul-ocidental do Gondwana e os ciclos de subsidência da Bacia do Paraná. *Revista Brasileira de Geociências*, *28*(4), 473-484.

Milani, E.J., Melo, J.H.G. de, Souza, P.A. De, Fernandes, L.A. & França, A.B. (2007). Bacia do Paraná. *Boletim de Geociências da Petrobras*, 8, 265–287

Mizusaki, A. M. P., Thomaz Filho, A., & De Cesero, P. (1998). Ages of the magmatism and the opening of the South Atlantic Ocean. *Pesquisas em Geociências*, *25*(2), 47-57.

Mohriak, W. U., Nóbrega, M., Odegard, M. E., Gomes, B. S., & Dickson, W. G. (2010). Geological and geophysical interpretation of the Rio Grande Rise, south-eastern Brazilian margin: extensional tectonics and rifting of continental and oceanic crusts.

Mohriak, W. (2012). Bacias da Margem Continental Divergente. *Geologia do Brasil.* São Paulo, Beca, 466-480.

Nürnberg, D., & Müller, R. D. (1991). The tectonic evolution of the South Atlantic from Late Jurassic to present. *Tectonophysics*, *191*(1-2), 27-53.

Oriolo, S., Oyhantçabal, P., Basei, M. A., Wemmer, K., & Siegesmund, S. (2016). The Nico Pérez Terrane (Uruguay): From Archean crustal growth and connections with the Congo Craton to late Neoproterozoic accretion to the Río de la Plata Craton. *Precambrian Research*, *280*, 147-160.

Oriolo, S., Oyhantçabal, P., Wemmer, K., & Siegesmund, S. (2017). Contemporaneous assembly of Western Gondwana and final Rodinia break-up: implications for the supercontinent cycle. *Geoscience Frontiers*, *8*(6), 1431-1445.

O'Sullivan, P. B., Murphy, J. M., & Blythe, A. E. (1997). Late Mesozoic and Cenozoic thermotectonic evolution of the central Brooks Range and adjacent North Slope foreland basin, Alaska: Including fission track results from the Trans-Alaska Crustal Transect (TACT). *Journal of Geophysical Research: Solid Earth*, *102*(B9), 20821-20845.

Oyhantçabal, P., Siegesmund, S., & Wemmer, K. (2011). The Río de la Plata Craton: a review of units, boundaries, ages and isotopic signature. *International Journal of Earth Sciences*, *100*(2-3), 201-220.

Oyhantçabal, P., Wagner-Eimer, M., Wemmer, K., Schulz, B., Frei, R., & Siegesmund, S. (2012). Paleo-and Neoproterozoic magmatic and tectonometamorphic evolution of the Isla Cristalina de Rivera (Nico Pérez Terrane, Uruguay). *International Journal of Earth Sciences*, *101*(7), 1745-1762.

Oyhantçabal, P., Oriolo, S., Philipp, R. P., Wemmer, K., & Siegesmund, S. (2018). The Nico Pérez Terrane of Uruguay and Southeastern Brazil. In *Geology of Southwest Gondwana* (pp. 161-188). Springer, Cham.

Parra, M., Mora, A., Sobel, E. R., Strecker, M. R., & González, R. (2009). Episodic orogenic front migration in the northern Andes: Constraints from low-temperature thermochronology in the Eastern Cordillera, Colombia. *Tectonics*, *28*(4).

Pérez-Díaz, L., & Eagles, G. (2014). Constraining South Atlantic growth with seafloor spreading data. *Tectonics*, *33*(9), 1848-1873.

Philipp, R. P., Machado, R., & Chemale Jr, F. (2003). Reavaliação e novos dados geocronológicos (Ar/Ar, Rb/Sr e Sm/Nd) do Batólito Pelotas no Rio Grande do Sul: implicações petrogenéticas e idade de reativação das zonas de cisalhamento. *Geologia USP. Série Científica*, *3*, 71-84.

Philipp, R. P., Pimentel, M. M., & Chemale Jr, F. (2016). Tectonic evolution of the Dom Feliciano Belt in Southern Brazil: geological relationships and U-Pb geochronology. *Brazilian Journal of Geology*, *46*, 83-104.

Ponte, F. C., & Asmus, H. E. (2004). As bacias marginais brasileiras: estágio atual de conhecimento. *Boletim de Geociências da Petrobras*, *12*(2), 385-420.

Quirk, D. G., & Rüpke, L. H. (2018). Melt-induced buoyancy may explain the elevated rift-rapid sag paradox during breakup of continental plates. *Scientific reports*, *8*(1), 1-13.

Rapela, C. W., Fanning, C. M., Casquet, C., Pankhurst, R. J., Spalletti, L., Poiré, D., & Baldo, E. G. (2011). The Rio de la Plata craton and the adjoining Pan-African/brasiliano terranes: their origins and incorporation into south-west Gondwana. *Gondwana Research*, *20*(4), 673-690.

Reiners, P. W. (2005). Zircon (U-Th)/He thermochronometry. *Reviews in Mineralogy and Geochemistry*, *58*(1), 151-179.

Reiners, P. W., & Farley, K. A. (2001). Influence of crystal size on apatite (U–Th)/He thermochronology: an example from the Bighorn Mountains, Wyoming. *Earth and Planetary Science Letters*, *188*(3-4), 413-420.

Reiners, P. W., Carlson, R. W., Renne, P. R., Cooper, K. M., Granger, D. E., McLean, N. M., & Schoene, B. (2017). *Geochronology and thermochronology*. John Wiley & Sons.

Riccomini, C., Velázquez, V. F., & Gomes, C. B. (2005). Tectonic controls of the Mesozoic and Cenozoic alkaline magmatism in central-southeastern Brazilian Platform. *Mesozoic to Cenozoic alkaline magmatism in the Brazilian Platform*, *123*, 31-56.

Rossello, E. A., de Santa Ana, H., & Veroslavsky, G. (2000). El lineamiento Santa Lucía-Aiguá-Merin (Uruguay): un corredor tectónico extensivo y transcurrente dextral precursor de la apertura Atlántica. *Revista Brasileira de Geociências*, *30*(4), 749-756.

Rossello, E. A., Veroslavsky, G., & Masquelin, H. (2007). El corredor Juro-Cretácico Santa Lucía–Aiguá–Merin (Uruguay): cinemática transcurrente dextral y controles preexistentes. *Revista de la Asociación Geológica Argentina*, *62*(1), 92-104.

Rossetti, L. M., Lima, E. F., Waichel, B. L., Scherer, C. M., & Barreto, C. J. (2014). Stratigraphical framework of basaltic lavas in Torres Syncline main valley, southern Parana-Etendeka Volcanic Province. *Journal of South American Earth Sciences*, *56*, 409-421.

Saenz, C. T., Hackspacher, P. C., Neto, J. H., Iunes, P. J., Guedes, S., Ribeiro, L. F. B., & Paulo, S. R. (2003). Recognition of Cretaceous, Paleocene, and Neogene tectonic reactivation through apatite fission-track analysis in Precambrian areas of southeast Brazil: association with the opening of the South Atlantic Ocean. *Journal of South American Earth Sciences*, *15*(7), 765-774.

Santos, J. O., Chernicoff, C. J., Zappettini, E. O., McNaughton, N. J., & Greau, Y. (2017). U-Pb geochronology of Martín García, Sola, and Dos Hermanas Islands (Argentina and Uruguay): Unveiling Rhyacian, Statherian, Ectasian, and Stenian of a forgotten area of the Río de la Plata Craton. *Journal of South American Earth Sciences*, *80*, 207-228.

Scherer, C. M. S. (2000). Eolian dunes of the Botucatu Formation (Cretaceous) in southernmost Brazil: morphology and origin. *Sedimentary Geology*, *137*(1-2), 63-84.

Scotese, C. R., Boucot, A. J., & McKerrow, W. S. (1999). Gondwanan palaeogeography and pal1 oclimatology. *Journal of African Earth Sciences*, *28*(1), 99-114.

Shuster, D. L., Flowers, R. M., & Farley, K. A. (2006). The influence of natural radiation damage on helium diffusion kinetics in apatite. *Earth and Planetary Science Letters*, *249*(3-4), 148-161.

Stica, J. M., Zalán, P. V., & Ferrari, A. L. (2014). The evolution of rifting on the volcanic margin of the Pelotas Basin and the contextualization of the Paraná–Etendeka LIP in the separation of Gondwana in the South Atlantic. *Marine and Petroleum Geology*, *50*, 1-21.

Tagami, T. (2005). Zircon fission-track thermochronology and applications to fault studies. *Reviews in Mineralogy and Geochemistry*, *58*(1), 95-122.

Tagami, T. (2012). Thermochronological investigation of fault zones. *Tectonophysics*, *538*, 67-85.

Teixeira, W., Renne, P. R., Bossi, J., Campal, N., & D'Agrella Filho, M. S. (1999). 40Ar–39Ar and Rb–Sr geochronology of the Uruguayan dike swarm, Rio de la Plata Craton and implications for Proterozoic intraplate activity in western Gondwana. *Precambrian Research*, *93*(2-3), 153-180.

Torsvik, T. H., Rousse, S., Labails, C., & Smethurst, M. A. (2009). A new scheme for the opening of the South Atlantic Ocean and the dissection of an Aptian salt basin. *Geophysical Journal International*, *177*(3), 1315-1333.

Turner, S., Regelous, M., Kelley, S., Hawkesworth, C., & Mantovani, M. (1994). Magmatism and continental break-up in the South Atlantic: high precision40Ar-39Ar geochronology. *Earth and Planetary Science Letters*, *121*(3-4), 333-348.

Vermeesch, P., (2009), RadialPlotter: a Java application for fission track, luminescence and other radial plots, Radiation Measurements, 44, 4, 409-410

Vermeesch, P. (2017). Statistics for LA-ICP-MS based fission track dating. *Chemical Geology*, *456*, 19-27.

Veroslavsky, G. (2003). Depósitos del Jurásico y Cretácico Temprano de la región meridional de Uruguay. El lineamiento Santa Lucia-Aiguá-Merin. *Cuencas sedimentarias del Uruguay: geología, paleontología y recursos naturales. Mesozoico. DIRAC-Facultad de Ciencias*, 115-140.

Wagner, G. A., Gleadow, A. J. W., & Fitzgerald, P. G. (1989). The significance of the partial annealing zone in apatite fission-track analysis: Projected track length measurements and uplift chronology of the Transantarctic Mountains. *Chemical Geology: Isotope Geoscience Section*, *79*(4), 295-305.

White, R., & McKenzie, D. (1989). Magmatism at rift zones: the generation of volcanic continental margins and flood basalts. *Journal of Geophysical Research: Solid Earth*, *94*(B6), 7685-7729.

Wildman, M., Brown, R., Beucher, R., Persano, C., Stuart, F., Gallagher, K., ... & Carter, A. (2016). The chronology and tectonic style of landscape evolution along the elevated Atlantic continental margin of South Africa resolved by joint apatite fission track and (U-Th-Sm)/He thermochronology. *Tectonics*, *35*(3), 511-545.

Will, T. M., & Frimmel, H. E. (2018). Where does a continent prefer to break up? Some lessons from the South Atlantic margins. *Gondwana Research*, *53*, 9-19.

Wolf, R. A., Farley, K. A., & Silver, L. T. (1996). Helium diffusion and low-temperature thermochronometry of apatite. *Geochimica et Cosmochimica Acta*, *60*(21), 4231-4240.

Wolf, R. A., Farley, K. A., & Kass, D. M. (1998). Modeling of the temperature sensitivity of the apatite (U–Th)/He thermochronometer. *Chemical Geology*, *148*(1-2), 105-114.

Yamada, R., Murakami, M., & Tagami, T. (2007). Statistical modelling of annealing kinetics of fission tracks in zircon; reassessment of laboratory experiments. *Chemical Geology*, *236*(1-2), 75-91.

Table 1: Summary of Zircon Fission Track results obtained for the Rio de La Plata Craton and the Dom Feliciano Belt, using the LA-ICP-MS method. Pooled and Central ages are reported, calculated using a primary zeta of 0,0401 ± 0,0005 based on Fish Canyon Tuff standard. N, number of crystals analyzed; χ2, chi-square probability of single population.

Sample #	Lat (°)	Long (°)	Elevation (m)	Lithology type	N #	Pooled age (Ma)	-95% (Ma)	+95% (Ma)	Central age (Ma)	±1σ (Ma)	χ2 (%)	Mean U (ppm)	Mean Th (ppm)	Mean Sm (ppm)
Rio de La Plata Craton														
Piedra Alta Terrane														
UY16	-34.06	-55.31	266	Granite	10	297.5	43	50	450	98	0	114.4	148.1	20.3
UY26	-34.10	-56.20	47	Granite	10	298.5	40	46	357	48	5	147.2	49.2	38.6
UY27	-33.96	-56.24	133	Granite	10	322.2	48	56	484	99	0	119.1	124.4	37.1
Tandilia Terrane														
UY18	-34.06	-55.31	266	Gneiss	8	337.4	53	63	385	46	50	84.6	74.5	15.0
UY19	-34.92	-56.17	150	Granite	10	354.1	58	69	426	48	37	28.7	20.7	16.1
Nico Pérez Terrane														
UY1	-31.89	-54.16	225	Granite	10	506.5	65	74	527	54	96	94.3	81.9	13.7
UY13	-33.28	-54.62	102	Granite	10	527.4	78	91	562	61	100	51.5	77.7	65.7
UY21	-34.41	-55.25	182	Granite	9	468.7	61	70	469	53	100	629.7	233.4	205.6
UY23	-34.81	-55.25	121	Syenite	10	489.2	59	66	487	50	100	70.2	51.5	46.2
Dom Feliciano Belt														
Pelotas Batholith														
RS04	-30.90	-52.06	107	Granite	10	464.2	65	75	479	54	100	61.4	59.4	19.3
RS07	-31.26	-52.34	284	Granite	10	450.3	59	67	494	69	3	115.5	104.0	15.4
RS10	-31.59	-52.51	190	Diorite	10	437.6	57	65	482	49	38	114.0	110.4	15.9
RS12	-31.03	-53.39	285	Granite	10	464.3	59	67	472	50	100	56.8	54.1	15.2
RS14	-31.46	-53.34	426	Granite	7	461.4	78	93	500	65	84	107.4	83.8	17.5
UY3	-32.62	-54.21	256	Mylonite	10	451.3	62	71	463	52	100	85.8	75.0	13.2
Cuchilla Dionísio Terrane														
UY29	-34.85	-54.63	7	Granite	10	530.5	64	73	550	56	46	94.3	81.9	13.7
UY30	-34.59	-54.12	3	Schist	10	311.6	46	53	321	37	100	69.7	47.6	10.3
UY32	-34.04	-53.54	4	Granite	10	254.3	37	43	280	31	67	104.8	89.4	16.4

Table 2: Summary of Apatite (U-Th)/He ages and parameters. Crystal dimensions were used to estimate an equivalent spherical radius. eU, total uranium content; Unc., uncorrected; Corr., corrected; Ft, alpha ejection factor for age correction (see Farley et al. 1996).

Apatite (U-Th)/He analyses																	
Sample #	Lat (°)	Long (°)	Elevation (m)	Lithology type	Crystal #	U (ppm)	Th (ppm)	Sm (ppm)	He (nmol/g)	eU (ppm)	Radius (µm)	Age Unc. (Ma)	Ft #	Age Corr. (Ma)	±2σ (Ma)	Ave. Corr. (Ma)	±2σ (Ma)
X1	-30.56	-52.45	440	Granite	1	36.24	53.85	82.63	34.82	49.05	39.40	128.7	0.621	207.2	12.4	217.7	22.4
					2	54.29	91.16	69.64	59.18	75.62	36.20	142.1	0.591	240.1	14.4		
					3	52.26	82.31	141.88	49.47	71.92	37.77	124.7	0.606	205.6	12.3		
X2	-31.15	-52.83	330	Granite	1	86.97	13.69	113.10	96.66	90.69	52.79	193.3	0.725	266.6	16.0	306.7	46.6
					2	28.22	2.35	87.74	39.19	29.20	46.50	241.1	0.693	347.4	20.8		
					3	58.24	5.33	106.28	69.09	60.01	44.42	208.3	0.681	306.1	18.3		

Highlights

First zircon fission-track ages for the Rio de La Plata Craton and Dom Feliciano belt

Data support an early Paleozoic cooling phase, after the Brasiliano/Pan-African Cycle

Protracted and complex thermal cooling of the region during Phanerozoic

Basement was near surface (T≤ 60°C) before Mesozoic rifting and West Gondwana breakup

Magmatism related to the Atlantic rifting had minor effect in basement temperature

Declaration of interests

☒ The authors declare that they have no known competing financial interests or personal relationships that could have appeared to influence the work reported in this paper.

☐The authors declare the following financial interests/personal relationships which may be considered as potential competing interests: